ELSEVIER

Palaeogeography, Palaeoclimatology, Palaeoecology 203 (2004) 207–237

PALAEO

www.elsevier.com/locate/palaeo

Causes and consequences of extreme Permo-Triassic warming to globally equable climate and relation to the Permo-Triassic extinction and recovery

David L. Kidder *, Thomas R. Worsley

Department of Geological Sciences, Ohio University, Athens, OH 45701-2979, USA

Received 29 November 2002; received in revised form 28 July 2003; accepted 6 October 2003

Abstract

Permian waning of the low-latitude Alleghenian/Variscan/Hercynian orogenesis led to a long collisional orogeny gap that cut down the availability of chemically weatherable fresh silicate rock resulting in a high-CO_2 atmosphere and global warming. The correspondingly reduced delivery of nutrients to the biosphere caused further increases in CO_2 and warming. Melting of polar ice curtailed sinking of O_2- and nutrient-rich cold brines while pole-to-equator thermal gradients weakened. Wind shear and associated wind-driven upwelling lessened, further diminishing productivity and carbon burial. As the Earth warmed, dry climates expanded to mid-latitudes, causing latitudinal expansion of the Ferrel circulation cell at the expense of the polar cell. Increased coastal evaporation generated O_2- and nutrient-deficient warm saline bottom water (WSBW) and delivered it to a weakly circulating deep ocean. Warm, deep currents delivered ever more heat to high latitudes until polar sinking of cold water was replaced by upwelling WSBW. With the loss of polar sinking, the ocean was rapidly filled with WSBW that became increasingly anoxic and finally euxinic by the end of the Permian. Rapid incursion of WSBW could have produced $\sim$20 m of thermal expansion of the oceans, generating the well-documented marine transgression that flooded embayments in dry, hot Pangaean mid-latitudes. The flooding further increased WSBW production and anoxia, and brought that anoxic water onto the shelves. Release of CO_2 from the Siberian traps and methane from clathrates below the warming ocean bottom sharply enhanced the already strong greenhouse. Increasingly frequent and powerful cyclonic storms mined upwelling high-latitude heat and released it to the atmosphere. That heat, trapped by overlying clouds of its own making, suggests complete breakdown of the dry polar cell. Resulting rapid and intense polar warming caused or contributed to extinction of the remaining latest Permian coal forests that could not migrate any farther poleward because of light limitations. Loss of water stored by the forests led to aquifer drainage, adding another $\sim$5 m to the transgression. Non-peat-forming vegetation survived at the newly moist poles. Climate feedback from the coal-forest extinction further intensified warmth, contributing to delayed biotic recovery that generally did not begin until mid-Triassic, but appears to have resumed first at high latitudes late in the Early Triassic. Current quantitative models fail to generate high-latitude warmth and so do not produce the chain of events we outline in this paper. Future quantitative modeling addressing factors such as polar cloudiness, increased poleward heat transport by deep water and its upwelling by cyclonic storms, and sustainable mid-latitude sinking of warm brines to promote anoxia,

* Corresponding author. Tel.: +1-740-593 1108; Fax: +1-740-593 0486.
E-mail address: kidder@ohio.edu (D.L. Kidder).

0031-0182/03/$ – see front matter
doi:10.1016/S0031-0182(03)00667-9

warming, and thermal expansion of deep water may more closely simulate conditions indicated by geological and paleontological data.

Keywords: greenhouse; Permian–Triassic extinction; anoxia; warm saline bottom water; storms

1. Introduction

We present a climate model of Earth system evolution from the Carboniferous and Early Permian icehouse to extreme Late Permian and Early Triassic greenhouse warmth. Although we are not the first to do so (see below), we suggest that the warming played a key role in causing the end-Permian extinction. The feedbacks proposed in our global warming model weakened ecosystems prior to the sudden and devastating extinction. Feedback from the extinction itself probably intensified unfavorable conditions, probably extending the unusually long Early Triassic recovery interval into the Late Scythian (Hallam, 1991; Erwin, 1998a,b).

The end-Permian extinction devastated both marine and terrestrial ecosystems (Erwin, 1993, 1994; Hallam and Wignall, 1997; Erwin et al., 2002; Wignall and Twitchett, 2002). A wide range of kill mechanisms has been proposed, but no clear consensus for any one extinction mechanism has emerged. Past suggestions include: niche loss during assembly of Pangaea (Valentine and Moores, 1970), cooling (Stanley, 1984), hyposalinity (Beurlen, 1956; Fischer, 1964; Stevens, 1977), volcanism (Renne et al., 1995; Kozur, 1998; Reichow et al., 2002), anoxia (Wignall and Hallam, 1992; Wignall and Twitchett, 1996); hypercapnia (Knoll et al., 1996); warming and acid rain via volcanism (Visscher et al., 1996), warming via methane release (Morante, 1996), extraterrestrial impact (Becker et al., 2001; Kaiho et al., 2001), and a combination of many of the above (Erwin, 1993). The extinction interval is now known to be quite short (Bowring et al., 1998), lasting less than half a million years, and its rapidity rules out some proposed mechanisms (Erwin et al., 2002).

Our model synthesizes a wide variety of Permian and Triassic factors including tectonics, climatic aspects of ocean and atmospheric circulation and chemistry, and terrestrial and marine biotas. Global systemic changes were set in motion as the final continental collisions associated with Pangaean assembly waned near the end of the Early Permian, resulting in a dearth of landmass collisions until the mid-Triassic. The consequence was a decline in silicate weathering and slowing of carbon burial that yielded a high atmospheric CO_2 content, intense global warming, and very low meridional temperature gradients as supported by warm-climate high-paleolatitude floras (Taylor et al., 1992; Retallack, 1999; Rees et al., 2002). Besides warming, climate consequences of high CO_2 include generally increased absolute atmospheric water vapor content, poleward moisture transport, and abundant rainfall at high latitudes (Manabe et al., 1994). Feedbacks from warming are consistent with many aspects suggested by previous workers such as latitudinal expansion of dry and warm conditions along with monsoonal tropics characterized the Late Permian and Early Triassic after the Gondwanan glaciers melted (e.g. Kutzbach and Gallimore, 1989; Kutzbach and Ziegler, 1993; Parrish, 1993; Ziegler et al., 1997; Retallack, 1999), and significant reduction in strength of ocean circulation (e.g. Fischer, 1964; Holser, 1977; Holser et al., 1989; Wignall and Twitchett, 1996; Isozaki, 1997; Hotinski et al., 2001).

Widespread Late Permian and Early Triassic anoxia (Wignall and Hallam, 1992, 1993; Isozaki, 1997; Hallam and Wignall, 1997; Wignall and Twitchett, 2002) is consistent with the prediction of the three-box model of Herbert and Sarmiento (1991) for a warm world with small temperature gradients between the equator and the poles relative to those of today. Models focused on generation of deep-ocean anoxia have quantified a number of mechanisms by which such anoxia may have developed (Sarmiento et al., 1988; Hotinski et al., 2000, 2001; Zhang et al., 2001). Tak-

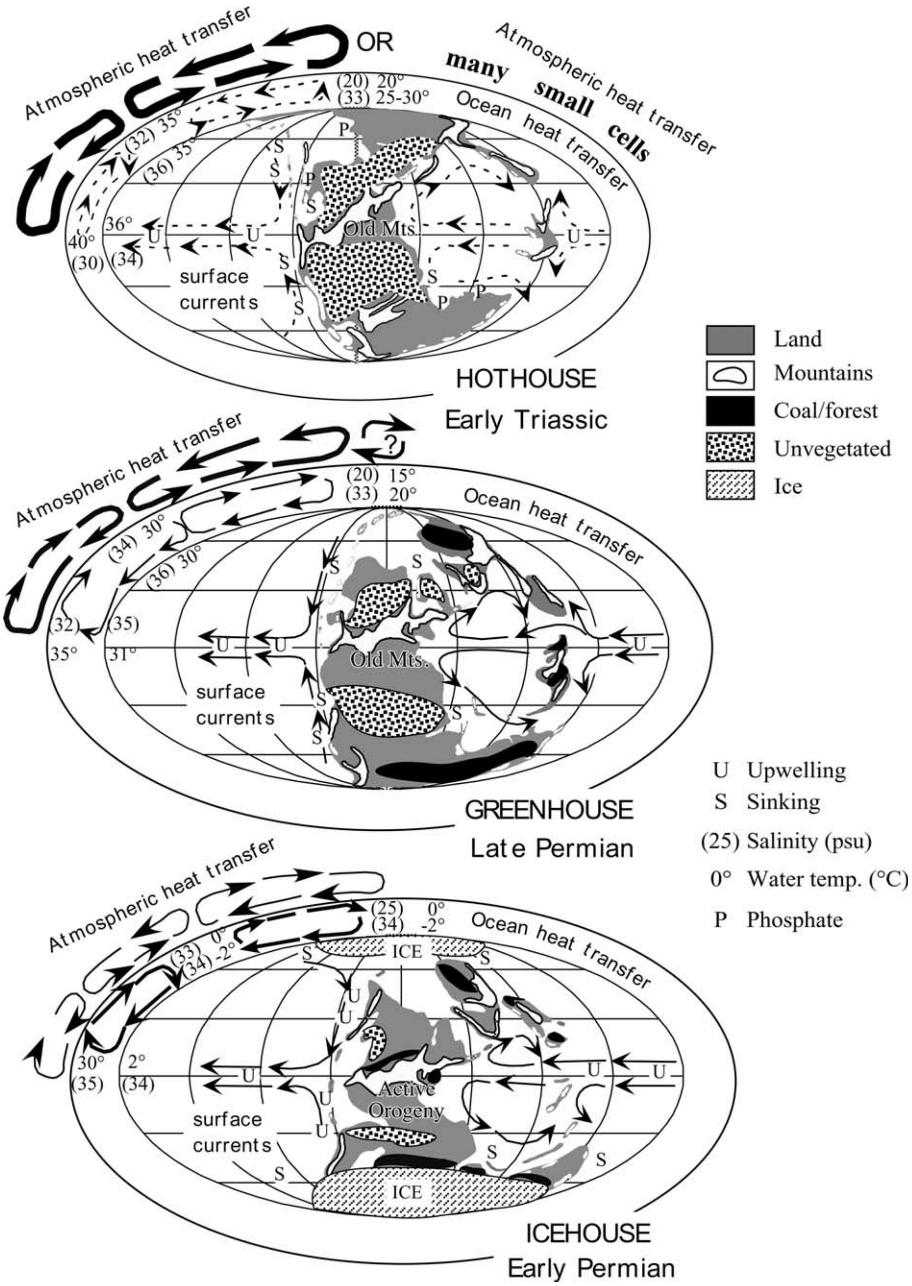

Fig. 1. Paleogeographic maps of three time slices pertaining to this study. Each map shows paleolandmass and mountain positions generated with the PGIS program written by C.R. Scotese. We interpret the active, low-latitude Alleghenian orogeny as a significant cooling factor in the Early Permian that lost effectiveness when the orogeny ended (see text for discussion). Features noted in key to symbols such as unvegetated regions (many of which may be deserts), coals and forests, and ice are modified from Erwin (1993) and Ziegler et al. (1997). Early Triassic phosphates are from Trappe (1994). Surface currents and upwelling and sinking areas are our estimates. Equal area projections are rimmed with our interpretations of ocean heat transfer and atmospheric heat transfer as discussed in the text (arrows). Postulated temperature and salinity values at the outside of the ovals represent the surface ocean whereas inward values represent the deep ocean. (A) Early Permian world in which active collisional orogenesis and extensive ice cover. It is assumed that these conditions are comparable to those of the modern icehouse world from which our numerical values are taken. (B) Late Permian. (C) Early Triassic.

Table 1
Sets of key aspects that describe the Permian and Triassic and serve as grounding for our model

Observation	Duration	Inferred cause/remarks	Selected references
Long-term changes in the Permian leading up to the extinction			
Reduction of activity in the Pangean low-latitude orogenic belt	tens of Myr	Waning of Pangean assembly	Windley (1995), Erwin (1993)
Decline in $^{87}Sr/^{86}Sr$	tens of Myr	Reduction in continental input	Burke et al. (1982), Denison et al. (1994)
Waning of Permo-Carboniferous glaciation	tens of Myr	Pangean assembly wanes	Crowell (1999), Moore and Worsley (1994), this paper
Rising atmospheric CO_2	tens of Myr	Pangean assembly wanes	Berner (1990), Ekart et al. (1999), this paper
Global warming	tens of Myr	Rising atmospheric CO_2 and CH_4	Berner (1990), Holser et al. (1989), Erwin (1993), Retallack (1999), this paper
Expansion of desert belts	tens of Myr	Warming and drying climate	Ziegler et al. (1997)
Retreat of floras to high latitudes	tens of Myr	Drying climate	Erwin (1993), Taylor et al. (1992), Ziegler et al. (1997), Rees et al. (2002)
Extensive evaporite deposition	~10 Myr	Warming and drying climate	Erwin (1993), Ziegler et al. (1997)
Declining atmospheric oxygen	tens of Myr	Reduction in photosynthetic activity	Berner and Canfield (1989), Graham et al. (1995), Berner (2001); this paper
Events temporally more closely correlated with the extinction			
Ocean anoxia	~20 Myr	Reduced ocean circulation	Wignall and Hallam (1992, 1993), Wignall and Twitchett (1996, 2002), Isozaki (1997)
Oceanic euxinia	~10 Myr	Reduced ocean circulation	Wignall and Hallam (1992, 1993), Wignall and Twitchett (1996, 2002), Isozaki (1997)
Transgression	~2 Myr	Tectonics (Hallam/Wignall refs) or Whole ocean thermal expansion and aquifer drainage (this paper)	Hallam (1991, 1999), Wignall and Hallam (1992, 1993), Hallam and Wignall (1999)
Expansion of shelf anoxia	~2 Myr	Transgression and increased ocean stratification	Wignall and Twitchett (1996, 2002)
Positive sulfur isotope shift	~10 Myr	Sinking $\delta^{34}S$-rich brines and/or organic burial of $\delta^{32}S$-rich pyrite	Holser (1977), Hallam and Wignall (1997), Broecker and Peacock (1999)
Increasing $^{87}Sr/^{86}Sr$	~10 Myr	cause unclear (see text)	Martin and Macdougall (1995), Korte et al. (2003)
Fungal Spore horizon	~1 Myr	Destruction of forests	Visscher et al. (1996), Erwin et al. (2002)
Siberian traps volcanism	~1 Myr		Makarenko (1976), Erwin (1993), Reichow et al. (2002)
Very rapid events			
End-Permian extinction	10^4 to 10^5 years	many proposed causes	Erwin (1993), Bowring et al. (1998), Erwin et al. (2002)
Negative $\delta^{13}C$ anomaly	10^4 to 10^5 years	Release of light carbon, productivity loss; ecosystem adjustment	Holser (1989); Erwin (1993), Broecker and Peacock (1999), Wignall (2001), Berner (2002)
Negative $\delta^{18}O$ anomaly	10^4 to 10^5 years	Warming	Holser et al. (1989)
Bolide impact?	geologically instantaneous		Becker et al. (2001), Kaiho et al. (2001)
Early Triassic gaps			
Chert gap	~10 Myr	nutrient shortage	Erwin (1993), Kidder and Erwin (2001)
Phosphate gap	~10 Myr	nutrient shortage (our interpretation)	Trappe (1994); this paper
Metazoan reef gap	thru Early Triassic	warmth, hypercapnia, hyposalinity	Fagerstrom (1987), Erwin (1993), Knoll et al. (1996)
Coal gap	~10 Myr	forest destruction and delayed recovery	Veevers et al. (1994); Retallack (1996)
Lycopod dominance	thru Early Triassic	recovery flora	Looy et al. (1999), Yaroshenko (1997)
Orogeny gap	Guadalupian to Anisian	lack of continental collisions	Veevers (1989), Erwin (1993); this paper
Disaster biota	References		
Examples of Early Triassic disaster taxa and selected references (see text for discussion)			
Stromatolitic reefs			Schubert and Bottjer (1992)
Acritarch swarms			Balme (1970), Hallam and Wignall (1997)
Cephalopods			Hallam and Wignall (1997)

Table 1 (*Continued*).

Observation	Duration	Inferred cause/remarks	Selected references
Lingulids			Rodland and Bottjer (2001)
Zooplankton (e.g. tintinnids)			Eshet (1992), Hallam and Wignall (1997)
Adult dwarf microgastropods			Hallam and Wignall (1997)
'Paper' clams (e.g. *Claraia*)			Hallam and Wignall (1997)
Epifaunal bivalves			McRoberts (2001)
Lystrosaurus			King (1990)
Lycopsids			Looy et al. (1999), Yaroshenko (1997)
Terrestrial burrowing networks			Miller et al. (2001)

en individually, quantitative model results either fail to generate sustainable anoxia (Zhang et al., 2001) or produce only dysoxia or weak anoxia (Hotinski et al., 2000, 2001). Our model suggests that the combined effect of these variables acting in concert was sufficient to generate the extensive anoxia and euxinia that characterized the latest Permian and Early Triassic.

The lack of an effective quantitative model for a poleward heat transport mechanism to maintain warm oceans at high latitudes during Cretaceous greenhouse climates (Haupt and Seidov, 2001) applies even more to the extreme high-latitude warmth (Taylor et al., 1992, 2000; Retallack, 1999; Sheldon and Retallack, 2002) of the Late Permian and Early Triassic. General circulation models that force increased global warmth by imposing high values of atmospheric CO_2 have not been able to produce Late Permian warm climates in high southern paleolatitudes that are suggested by paleobotanical data (Rees et al., 1999, 2002; Gibbs et al., 2002). The lack of a warm polar surface current in the models has been suggested as a possible reason for this deficiency in the model results (Ziegler, 1998). In contrast, our model calls for poleward heat transport by warm deep-ocean brines (Chamberlin, 1906; Brass et al., 1982; Zhang et al., 2001; Bice and Marotzke, 2002). We further suggest that Ekman transport upwelling caused by cyclonic storms also warmed high latitudes as they mined warmth from deep brines and delivered it as latent heat to polar regions. Greatly increased cloud cover helped to maintain polar warmth, both from condensation and the heat retention provided by the clouds. Previous Permo-Triassic models do not predict either the storminess or heat-trapping polar cloudiness we propose.

Early Triassic extreme warmth rivals and perhaps exceeds that of the Late Paleocene thermal maximum that is suggested to have resulted from elevated atmospheric CO_2 and CH_4 (e.g. Zachos et al., 1993; Katz et al., 1999; Bice and Marotzke, 2002). High methane values have also been suggested for the Early Triassic (Erwin, 1993; Morante, 1996; Krull and Retallack, 2000; Sheldon and Retallack, 2002). The Early Triassic has other partial analogs in Earth history. For example, mid-Cretaceous warmth and anoxia was accompanied by lows in chert and phosphate accumulation (Hein and Parrish, 1987; Kidder and Erwin, 2001; Cook and McElhinny, 1979). The Early Silurian also has a phosphorite gap (Cook and McElhinny, 1979), a possible chert gap (Kidder and Erwin, 2001), it followed a significant extinction, and the Silurian has been suggested as a significant greenhouse (Worsley and Kidder, 1991). Mesoproterozoic drawdown of atmospheric CO_2 was probably minimized by some factors similar to those in the Early Triassic. Silicate weathering was limited by a paucity of orogenic activity and by the absence (Mesoproterozoic) and scarcity (Early Triassic) of terrestrial vegetation, which also minimized terrestrial photosynthetic CO_2 drawdown and consequent carbon burial. The Early Triassic euxinic ocean (e.g. Hallam and Wignall, 1997) somewhat resembled sulfidic Mesoproterozoic oceans characterized by weakly oxygenated surface waters (Canfield, 1998; Anbar and Knoll, 2002).

2. The Permo-Triassic world

2.1. Late Permian/Early Triassic warming and oxygen decline

The Permo-Carboniferous icehouse of Pangaea was analogous to the Cenozoic one in a number of respects, and so it serves as a useful starting point for consideration of Permo-Triassic climate change. Permo-Triassic continents were longitudinally arrayed into a sliceworld (Worsley and Kidder, 1991), although Pangaea was a single landmass in contrast to the two major slices of the modern world. Drawdown of CO_2 via chemical weathering of fresh silicate rock generated in active low-latitude orogenic belts was probably an effective cooling mechanism in both icehouses, and this mechanism has been suggested for initiation of Permo-Carboniferous glaciation (Moore and Worsley, 1994; Saltzman et al., 2000). The Alleghenian/Variscan/Hercynian orogenies that completed the unification of Gondwanaland and Laurasia (Fig. 1) were at least two and perhaps five times larger in areal extent than the modern Himalayan system which has been commonly suggested as the trigger for Cenozoic glaciation (e.g. Raymo, 1991). Andean-type tectonics have been ongoing along the Panthalassa-Pacific rim since at least the Late Paleozoic. Both worlds are marked by significant continental glaciers in the south polar region, and minimal Early Permian north polar landmasses probably resulted in a cap of frozen sea ice. Carboniferous and Early Permian ocean circulation probably approximated that of the Tertiary to Recent icehouse in that sinking cold, O_2-rich brines generated from the freezing of sea ice adjacent to the southern ice sheets were the dominant factor in pole-driven thermohaline circulation. Carbon burial by widespread coniferous and glossopterid forests probably contributed significantly to cooling as did photosynthetic drawdown of CO_2 and carbon burial by oceanic plankton in a well-mixed ocean receiving abundant nutrient runoff from the predominantly low-latitude orogenic belts.

The combined efforts of many workers (Table 1; Fig. 2) establish a baseline of Early Permian icehouse characteristics and the Late Permian and Early Triassic conditions toward which we extrapolate in our semi-quantitative model. Numerical values from the Cenozoic icehouse are used to approximate the Permo-Carboniferous icehouse (Table 2).

We propose that if the onset of Gondwanan glaciation was triggered by orogenesis, warming climates should be a consequence of the cessation of that cooling mechanism. Independent evidence exists for rising levels of atmospheric greenhouse gases and warmth during and after the melting of the Gondwanan ice sheets. A late Early Permian (Leonardian) rise in atmospheric CO_2 estimated from $\delta^{13}C$ pedogenic carbonate analyses (Ekart et al., 1999; Montanez et al., 2001) is consistent with the timing of glacial melting near the end of Pangaean orogenic assembly (Fig. 2). A decline in leaf stomate density in the Late Permian and Early Triassic from higher Early Permian values (Retallack, 2001) also supports increased atmospheric CO_2 in a similar fashion to post-Cretaceous results (Beerling et al., 2002). Model results (e.g. Berner, 1990, 1991, 2002) also support rising atmospheric CO_2 levels in the Late Permian and

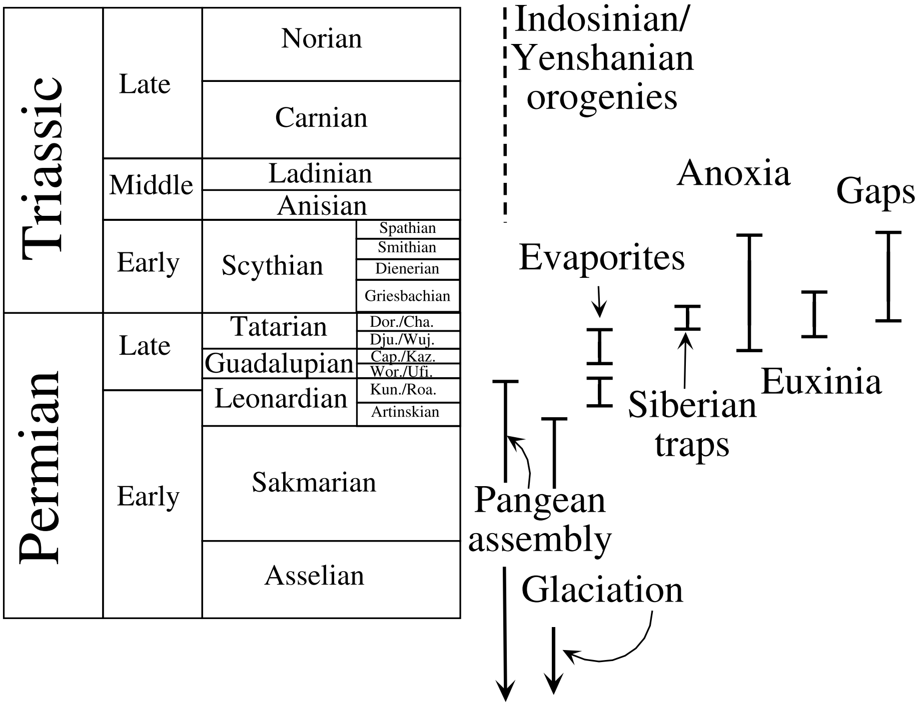

Fig. 2. Permo-Triassic time scale on which durations of key factors pertaining to the genesis of our model are portrayed. Compiled from Erwin (1993), Isozaki (1997), and Veevers (1989). See Table 1 for more factors and further explanation.

Early Triassic. Following glaciation, Late Permian expansion of desert belts, red beds, eolian dunes, and areas of evaporite formation coincided with a general retreat of forested areas toward high latitudes (Erwin, 1993; Parrish, 1993; Ziegler et al., 1997; Taylor et al., 1992; Retallack, 1999; Rees et al., 2002). The loss of forests (Erwin, 1993; Visscher et al., 1996; Rees et al., 2002), the Siberian traps volcanism (Makarenko, 1976; Erwin, 1993; Reichow et al., 2002), and clathrate release (e.g. Erwin, 1993; Morante, 1996) would all have led to increased atmospheric CO_2. Veevers et al. (1994) interpreted the herbaceous *Dicroidium* flora and its associated redbed facies as representative of warm climates in the Early Triassic following the cooler Permian association of *Glossopteris* and coal. Warm climates are inferred from sail fins on pelycosaurs that are now thought to have expelled body heat (Bennett, 1996) in contrast with earlier work that suggested the sail fins served as heat collectors (Haack, 1986). Scarcity of Late Permian charcoal suggests that despite dry conditions, Permian fires were not only rare (Scott, 2000; Wang, 1993, 2000), but consisted mostly of low-temperature surface and litter fires rather than full-scale crown forest fires (Scott, 2000). In addition to enhancing climate equability, melting ice sheets would have drowned small landmasses such as South China where the best marine record of the latest Permian and early Triassic is preserved.

Suggestions of Late Permian cool climates are not unknown. Stanley (1984, 1988) suggested cooling and possibly even glaciation in the latest Permian to explain the end-Permian extinction, but the glacial deposits cited by Stanley turned out to be Guadalupian (Erwin, 1993). Biogenic cherts used to suggest cool Late Permian climates (Beauchamp and Baud, 2002) could also reflect availability of nutrients and silica from our predicted high-latitude upwelling rather than temperature, but cold, temperate climates may well have characterized Late Permian polar regions. Kozur (1998) also used siliceous faunas to suggest cool-

Table 2
Postulated orogenic, orographic, atmospheric, and oceanic changes from the Early Permian through the Early Triassic

Model Predictions	Today and Early Permian	Late Permian	Early Triassic	References and comments
1. Orogeny	1 [A]	1/2 [A]	1/2 [A]	subduction orogeny continues; continent collision ceases
2. Atmospheric carbon dioxide	1 [A]	10 [B]	32 [C]	Assumes CO^2 is sole greenhouse gas which doubles for each 3°C rise in temperature (e.g. Worsley and Kidder (1991)
3. Polar ocean surface temperature	0°C [A]	15°C [B]	20°C [C]	Temperature based on high-latitude, warm-climate floras in the Late Permian(Taylor et al. (1992) and Middle Triassic (Retallack, 1999)
4. Equatorial ocean surface temperature	30°C [A]	35°C [B]	40°C* [C]	*postulated to preserve a reasonable pole-equator temperature gradient for Retallack's (1999) 'post apocalyptic greenhouse.'
5. Average global temperature	15°C [A]	25°C [B]	30°C [C]	A simple numerical average of polar and equatorial temperatures
6. Global SVP	1 [A]	2 [C]	2.8 [C]	SVP doubles for each 10°C increase
7. Proportion of equator-to-pole heat transport between ocean currents and atmosphere	~50% [A]	~80% [B]	>90% [C]	Wells (1997) Increased SVP and storm intensity plus weakened ocean currents favors higher atmospheric heat transport
8. Atmospheric poleward heat transport	1/2 [B]	1 1/4 [C]	1 1/2 [C]	Estimate for today is from Wells (1997) who further estimates that ~90% of today's atmospheric transport is via latent heat
9. Oceanic poleward heat transport	1/2 [B]	1/2 [C]	1/2 [C]	Deep-ocean circulation reverses direction as mid-latitude warm, saline bottom water replaces polar bottom water. Large storms can mine this heat even at high latitude
10. Total poleward heat transport	1 [A]	1 3/4 [C]	2 [C]	Large cyclonic storms that mine heat from a warm deep ocean will enhance poleward heat transport
11. Planetary windbelt speeds	1 [A]	2/3 [B]	2/3 [B]	Wind belt speed is proportional to pole-equator temperature gradient
12. Wind shear	1 [A]	4/9 [B]	4/9 [B]	Wind shear is proportional to square of velocity (Wells, 1997)
13. Ocean current speed	1 [A]	4/9 [B]	4/9 [B]	Ocean current speed is proportional to wind shear (Wells, 1997)
14. Wind-driven upwelling	1 [A]	4/9 [B]	4/9 [B]	Upwelling is proportional to wind shear (Wells, 1997)
15. Polar surface ocean salinity	25‰ [A]	20‰ [C]	20‰ [C]	Without a polar cell, frequent and intense storm activity freshens polar surface water
16. Polar deep-ocean salinity	34‰ [A]	33‰ [C]	33‰ [C]	Evaporation from expanded desert belt areas produces warm, saline bottom water that upwells at the poles (see Brass et al., 1982)
17. Equatorial surface ocean salinity	35‰ [A]	32‰ [C]	30‰ [C]	Frequent and intense storm activity freshens tropical surface waters, especially near continents
18. Equatorial deep-ocean salinity	34‰ [A]	35‰ [C]	34‰ [C]	Evaporation from expanded desert belt areas produces warm, saline bottom water
19. Whole ocean salinity	35‰ [B]	34‰ [C]	33‰ [C]	Ice cap melting and salt extraction could have lowered salinity by as much as 5‰ (Holser, pers. comm. cited in Horita et al., 1991). The simple numerical average of equal volume, 1-km-thick polar and equatorial mixed layers, and 3-km-thick polar and equatorial deep layers.
20. Moisture transport to continental interiors (see Fig. 7)	1 [A]	2/3 [B]	2/3 [C]	Moisture transport is proportional to wind speed and is dependent on height of coastal mountains, vegetation, and continent size. Pangean interior would be difficult to moisturize.
21. Monsoon intensity and frequency	1 [A]	1/2 [B]	?1/4 [C]	Monsoon intensity is proportional to global temperature and humidity, but is inversely proportional to mountain height (An et al., 2001). We think mountain height dominates the monsoon, but it is difficult to assess the effect of braided stream runoff across a minimally vegetated landscape
21. Aridity and runoff efficiency	1 [A]	2 [B]	4 [C]	Loss of wind speed promotes interior aridity. Loss of forests destroys soil/biomass moisture storage and yields braided streams

Table 2 (*Continued*)

Model Predictions	Today and Early Permian	Late Permian	Early Triassic	References and comments
22. Storm frequency and intensity	1 [A]	?1.5 [B]	?2 [C]	Storm frequency and intensity are proportional to temperature and SVP.
23. Polar penetration of storms	1 [A]	?3 [B]	?10 [C]	Late Permian and Early Triassic storms mine heat from warm, deep oceans. Early Permian storms are limited by cold water below the thermocline.
24. Photosynthetic oxygen production	1 [A]	?1/2 [B]	?1/4 [C]	Sharp drop in upwelling coupled with great loss of terrestrial flora.
25. Atmospheric oxygen	1 [A]	0.9 [A]	0.8 [A]	Frequency and type of fire (Scott, 2000). Models by Berner and Canfield (1989), Graham et al. (1995), Berner (2001). Oxidation of CH_4 and volcanic SO_2.
26. Ocean oxygen saturation	1 [A]	1/2 [A]	1/2 [A]	Oxygen solubility is inversely proportional to ocean temperature.
27. Ocean oxygen content	1 [A]	?1/2 [B]	?1/10 [B]	Widespread anoxia and euxinia (Wignall and Hallam, 1993; Hallam and Wignall, 1997; Isozaki, 1997)

For value estimates, today's value is defined as 1 unit. Letters in brackets indicate relative confidence of estimates: [A] = Strong: based on direct measurement or analog. [B] = Moderate: derived from an [A] estimate and in good agreement with other parameters. [C] = Weak: based on extrapolation, but consistent with other parameters.

ing. Ostracods as evidence of cool conditions (Kozur, 1998) could alternatively reflect salinity changes. The conodonts discussed by Kozur (1998) do not necessarily indicate cool waters (Wignall and Twitchett, 2002). The only geochemical evidence for latest Permian cooling is based on light $\delta^{13}C$ from one pedogenic carbonate locality that was used to suggest a reduction in atmospheric CO_2 in the latest Permian (Ekart et al., 1999; Montanez et al., 2001). Stone-rolls (Conaghan et al., 1994; Krull, 1999; Retallack, 1999) suggest cold temperate, but not necessarily glacial climates at high paleolatitudes.

Extremely warm Early Triassic climates were suggested by Dickins (1993). More recent work in terrestrial systems includes high-latitude paleosols (60°–85°S) that are typical of warm climate soils that characterize modern latitudes some 25–40° lower (Retallack, 1999). Paleosol studies suggest high atmospheric methane based on microbial evidence (Krull and Retallack, 2000), and on berthierine nodules that may have formed in reducing environments as large amounts of CH_4 oxidized to CO_2 (Sheldon and Retallack, 2002). These are consistent with the methane that Erwin (1993) invoked to help explain the $\delta^{13}C$ anomaly (Table 1), although the regression he calls for to explain the hydrate-release happened too early to explain the sudden $\delta^{13}C$ excursion.

Several lines of evidence and reasoning support declining atmospheric oxygen levels through the Late Permian and into the Early Triassic. A marked increase of anoxic marine sediments in the Late Permian intensified to euxinic conditions from latest Permian into the Early Triassic in both shelf and basinal settings (Wignall and Hallam, 1992, 1993; Wignall and Twitchett, 1996; Isozaki, 1997). Modeling results support a decline in atmospheric oxygen through this interval (Berner and Canfield, 1989; Graham et al., 1995; Berner, 2001), and berthierine nodules in earliest Triassic Antarctic paleosols (Sheldon and Retallack, 2002) support low atmospheric O_2 conditions. Scarce Late Permian charcoal could reflect lower atmospheric oxygen levels and/or less available wood to burn. The retreat of forests to smaller land areas at high latitudes (e.g. Erwin, 1993; Rees et al., 2002) would have sharply reduced terrestrial production of atmospheric oxygen. High levels of latest Permian and Early Triassic methane (Erwin, 1993; Krull and Retallack, 2000; Sheldon and Retallack, 2002) would have lowered atmospheric oxygen via oxidation to CO_2. Similarly, the large amounts of SO_2 emitted from the Siberian traps (Makarenko, 1976; Reichow et al., 2002) would have consumed atmospheric oxygen during oxidation to sulfate. The lesser volcanic H_2S component (Delmelle and Stix, 2000) would also contribute to atmospheric oxygen reduction.

2.2. The Permo-Triassic extinction

The rapid end-Permian extinction was preceded by an earlier extinction at the end of the Middle Permian (Stanley and Yang, 1994; Hallam and Wignall, 1997; Erwin et al., 2002). Erwin (1993) suggested that up to 70% of existing marine species went extinct by the end of the Guadalupian. Although loss of marine life ranged across many taxa, it exhibits a selective nature. Especially hard hit were shallow water dwellers including reefs, epifauna, suspension feeders, planktonic larvae, and plankton consumers (Erwin, 1993). Most reef types were affected as were $\sim$75% of fusulinid forams and their algal symbionts (Hallam and Wignall, 1997). Warmth may have selectively eliminated algal symbionts (coral bleaching). Selectivity of Late Permian extinctions has also been attributed to hypersalinity in desert belts, and sharply alternating seasonal surface salinity in the tropical monsoon areas (Fischer, 1964; Beurlen, 1956; Stevens, 1977). The high Changxingian extinction level of 81% of organisms with heavily calcified skeletons, lack of gills, weak internal circulation, and low metabolic rates was suggested by Knoll et al. (1996) to have resulted from hypercapnia. Contrastingly, only about 38% of organisms with active gills, active internal circulation, and high metabolic rates suffered Changxingian extinction. We suggest anoxia as an alternative or additional mechanism to hypercapnia for this selective aspect of the extinction.

Although it has long been accepted that the end-Permian extinction wiped out more marine families, genera, and species than any other extinction in Earth history, it is now clear that the event affected a broad range of both terrestrial and marine ecological niches (Hallam and Wignall, 1997; Twitchett et al., 2001; Erwin et al., 2002). The Siberian traps that straddle the Permo-Triassic boundary (Reichow et al., 2002) must also have introduced considerable global stress by rapidly expelling huge amounts of CO_2 and SO_2. The appearance of end-Permian fungal spores that Visscher et al. (1996) suggested as a possible consequence of sudden forest destruction by the volcanism are now known to have developed over the last million years of the Permian in China (Erwin et al., 2002), and before the boundary in Svalbard (Wignall et al., 1998) and probably in Australia (Michaelsen, 2002). Forest destruction without burning is consistent with low atmospheric oxygen discussed earlier. Non-combustive oxidation of the terrestrial biosphere at the Permo-Triassic boundary further elevated already high atmospheric CO_2 levels and reduced already low atmospheric oxygen levels.

3. Icehouse to greenhouse model

We propose a system of feedbacks that increased atmospheric CO_2 and warmed the world from the Permo-Carboniferous icehouse to a greenhouse that intensified through the Late Permian and into the Early Triassic (Fig. 3). Table 2 approximates the progressive changes in climatic parameters that led to the Early Triassic supergreenhouse. Late Permian increases in atmospheric carbon dioxide can be explained by three critical mechanisms (Figs. 1, 3 and 4). These are: (1) waning and ending of the orogenic activity that assembled Pangaea, (2) reduction in terrestrial photosynthetic CO_2 drawdown as forests diminished, and (3) reduction in CO_2 drawdown by nutrient-deficient and oxygen-starved oceanic plankton. In turn, all three are linked to a pronounced weakening of the planetary windbelt system and a consequent increase in heat transport via warm saline bottom water (WSBW) and increases in both frequency and intensity of cyclonic storms to mine WSBW heat (Table 2; Figs. 1 and 5).

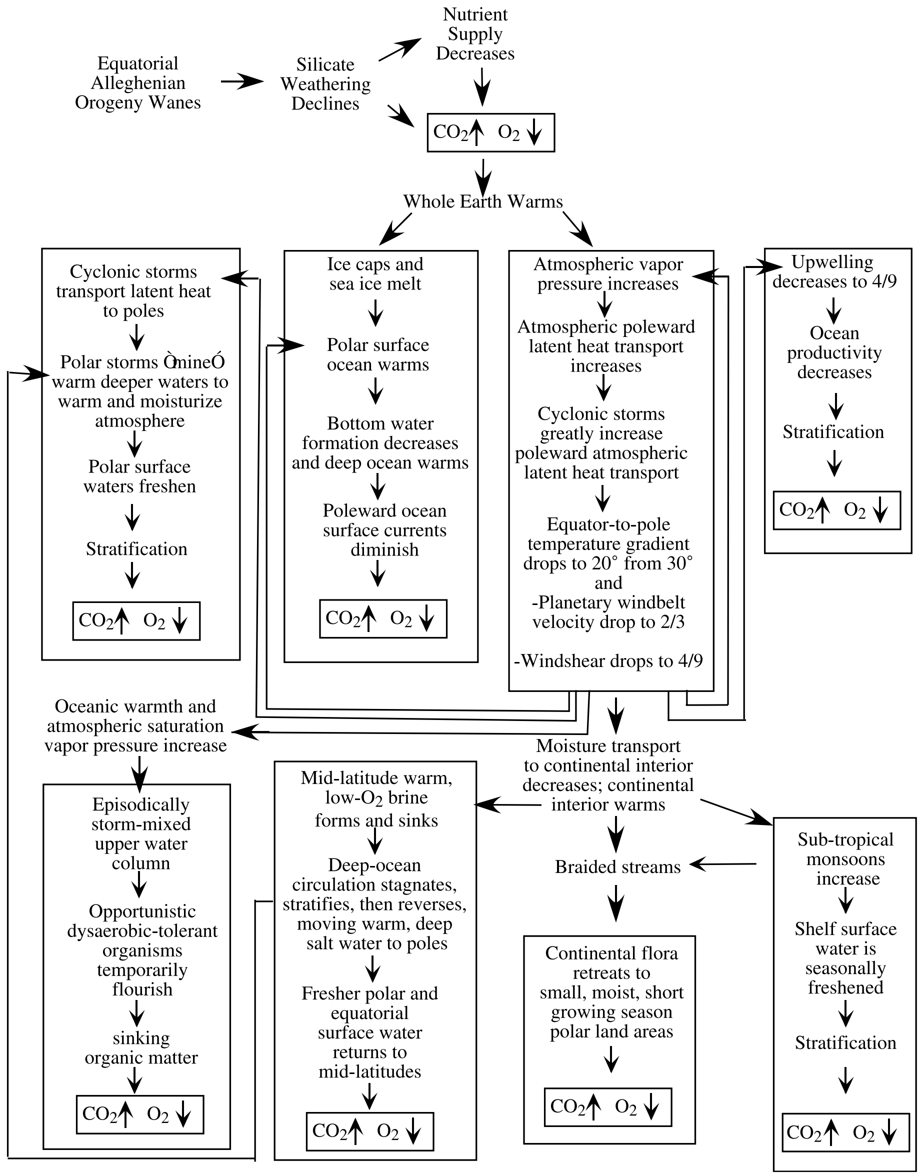

Fig. 3. Flow chart illustrating expected feedback relationships among processes that we predict for evolution of climate. The underlying assumption is that the Early Permian icehouse was a climatic regime comparable to that of today. From that starting point, the flow chart incorporates a wide range of predicted feedbacks that are explained in further detail in Table 2 and the text.

3.1. Reductions in CO_2 drawdown

Declining CO_2 drawdown is expected as the Pangaea-assembling Alleghenian, Hercynian, and Variscan low-latitude orogenies waned and the volume of readily weatherable silicate rock diminished. Warming and melting of the Gondwanan ice sheets are a logical consequence of those declines (Figs. 1, 3 and 4). The record of $^{87}Sr/^{86}Sr$ beginning in the late Carboniferous (e.g. Denison

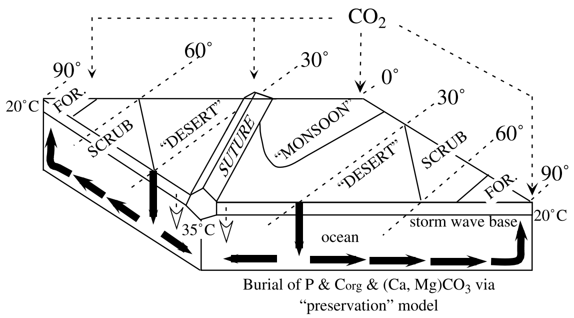

Early Triassic

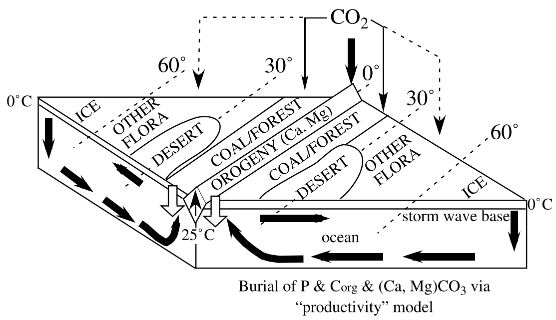

Early Permian

Fig. 4. Model diagram that illustrates the general differences between the icehouse conditions of the Early Permian vs. the greenhouse of the Early Triassic. Arrows in atmosphere show regions of CO_2 drawdown with thick solid arrows showing the most intense drawdown (e.g. Early Permian low-latitude orogeny) and dashed arrows showing weakest drawdown. Unfilled arrows show burial of phosphorus and carbon. Solid arrows in oceans show dominant direction of heat transport with the Early Permian resembling the modern icehouse and the Early Triassic oceanic heat transport driven by mid-latitude sinking of brines.

et al., 1994) is consistent with this expectation, particularly during a significant drop in the Sr ratio in the Leonardian and Guadalupian.

Further reduction in CO_2 drawdown is expected to have resulted from global reconfiguration of Late Permian forests. Loss of resident water as mid-latitude dry regions expanded (Fig. 1) also lessened silicate weathering. Saturation vapor pressure (SVP) doubles with each 10°C rise in temperature (e.g. Barron, 1989) so that we fully expect that increased atmospheric moisture content rose during late Permian warming with a concomitant increase in latent heat transport. However, relative humidity (VP/SVP) probably behaved differently, increasing at the equator and polar regions where warm moist air was ascending (Manabe et al., 1994), and decreasing in mid-latitudes, where cooler dry air was descending. Corresponding cloudiness and precipitation (Fig. 6) along with warmth were probably important sustaining factors for the high-latitude Late Permian Pangaean forests described by previous workers. (Erwin, 1993; Parrish, 1993; Ziegler et al., 1997; Taylor et al., 1992, 2000; Retallack, 1999; Rees et al., 2002). The effectiveness of silicate weathering in the much larger land area that was left unvegetated by the retreat (Fig. 1) was reduced because plant root systems intensify surface weathering by breaking up rock to generate soil and humus. Vegetation both increases available weatherable surface area and retains water that intensifies weathering reactions (Algeo et al., 1995; Berner and Berner, 1996; Algeo and Scheckler, 1998) given sufficient relief for physical removal of chemically inert materials (e.g. Stallard, 1985; Drever, 1994). Transpiration generates its own microclimate that promotes atmospheric moisture transport into continental interiors (Fig. 7). Heavy, seasonal rainfall in unforested and monsoonal Late Permian Pangaean tropical climate (Kutzbach and Gallimore, 1989; Kutzbach and Ziegler, 1993; Parrish, 1993) would, without forests, run off too rapidly to contribute significantly to chemical weathering (Fig. 7). The small land area covered by forests on small, tropical landmasses (Fig. 1) and at high Late Permian latitudes would not contribute significantly to CO_2 drawdown, and light limitation would have curtailed high-latitude forest productivity. Diminished terrestrial organic carbon burial is a further consequence of forest reduction.

Reductions in terrestrial nutrient input to oceans would be an additional consequence of diminished silicate weathering. Warming would have intensified as weaker upwelling from deep waters (Table 2; Fig. 5) delivered fewer nutrients to surface waters. Even if weakly upwelling deep anoxic waters bore high nutrient levels (e.g. Van Cappellen and Ingall, 1994), the anoxia of the upwelled waters (e.g. Wignall and Twitchett, 1996, 2002) could have prevented their efficient use. In our view, nutrient limitation lowered pho-

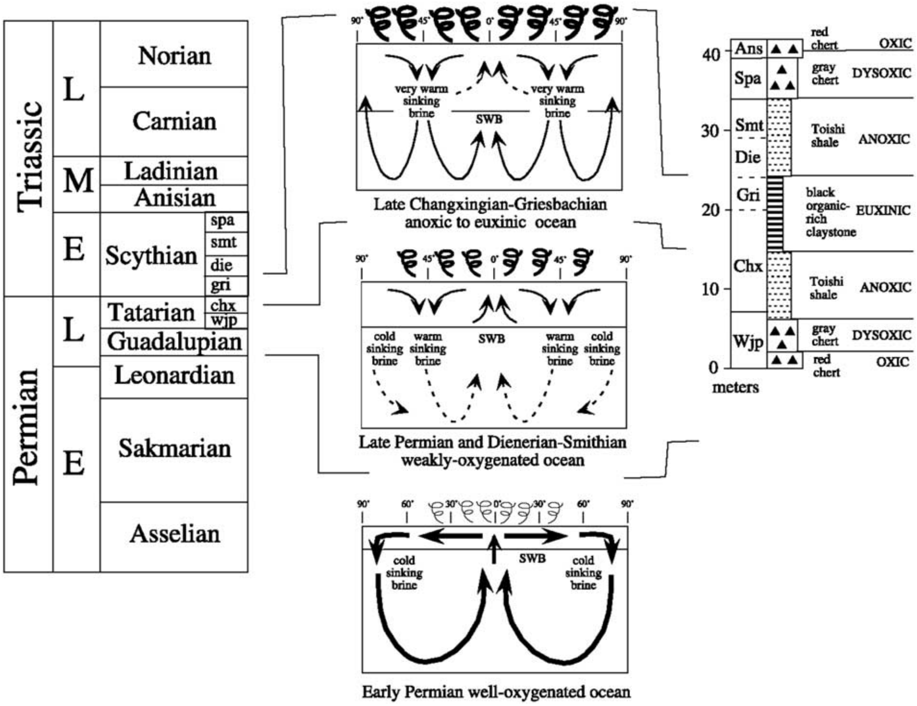

Fig. 5. Modeled changes in general nature of atmospheric circulation, thermohaline circulation, and dominant directions of surface water transport for Early Permian, Late Permian, and Early Triassic. Early Permian conditions are assumed to have been comparable to those of today. Line thickness and continuity is proportional to intensity of heat transport process. Cyclonic storm intensity and frequency are predicted to have risen through time along with storm wave base. The atmosphere became increasingly important as a heat transport mechanism as storms moved warm, humid air over oceans poleward from the equator.

tosynthetic plankton productivity and thus drawdown and burial of carbon.

Model CO_2 values (Berner, 1990, 1991) are consistent with warm climates, and the sharp changes in $\delta^{13}C$ and $\delta^{18}0$ (Table 1) support dramatically increased CO_2 and warming at the Permo-Triassic boundary (Berner, 2002). Recent computer models for Late Permian and Early Triassic climate assume high atmospheric CO_2 values on the order of 8× those in the modern world (e.g. Rees et al., 1999). Our postulated 25°C global temperature average for the late Permian (35° at the equator and 15° at the poles) suggests CO_2 levels ∼10× those of today. Evaluation of our suggested Early Triassic 30°C global temperature average (40° at the equator and 20° at the poles) by the Worsley and Kidder (1991) CO_2-temperature model suggests that atmospheric CO_2 could have exceeded 30× present values if it were the only greenhouse gas contributing to Early Triassic warmth. Alternative modeling by Berner (2002) weaves together the effects of four factors to raise Late Permian CO_2 levels to higher Early Triassic ones. He suggests that release of methane and its subsequent oxidation to CO_2 would have raised atmospheric CO_2 by 1.25× previous levels. An additional ∼1.25× increase would have resulted from mass mortality. Two approximate doublings of atmospheric CO_2 levels, one from the Siberian traps, and the other from carbon cycle reorganization would have combined with the other two factors to raise atmospheric CO_2 as much as 6×. Because these increases could buffer one another to some extent, we adopt a more conservative four-fold increase. The relation of Worsley and Kidder (1991) equates doubling of CO_2 from any arbitrary value with a 3°C temperature rise and a 10-fold CO_2 increase to a 10°C rise. The 4-fold CO_2 rise at the Permo-Triassic boundary would, therefore, yield a ∼6°C rise in global tem-

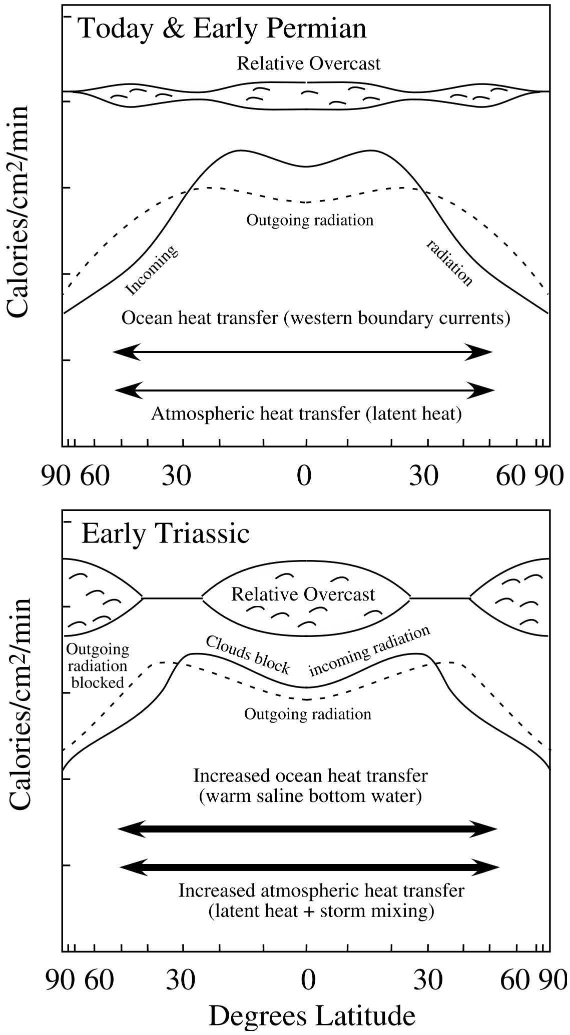

Fig. 6. Idealized schematic view of global energy balance differences between today (and Early Permian) and the Early Triassic. Early Triassic greenhouse poleward heat transport is increased (thicker arrows) via warm, saline bottom water and by heat mining of those waters by cyclonic storms (Fig. 5) that increase atmospheric transport of latent heat. A rise in SVP and poleward moisture transport as well as increased high-latitude rainfall are predicted consequences of atmospheric CO_2 enrichment (Manabe et al., 1994). See text for further explanation.

perature, which is consistent with the 5°C rise suggested from $\delta^{18}O$ results (Holser et al., 1989).

The modern-like Permian CO_2 value of 300 ppmV that Berner (2002) used as a baseline for his modeling yields a global average temperature of 15°C. We believe that these values represent the Early Permian icehouse and are too low for the Late Permian. The forests had, by the ice-free Wordian (Middle Permian), already moved to high latitudes (Rees et al., 2002), hence our suggested Late Permian global average temperature of 25°C. Our suggestion for 10× more than modern CO_2 levels in the Late Permian, or about 3000 ppmV, is in line with the values used by Rees et al. (1999) of 8× present atmospheric CO_2 levels in their model. The four-fold increase (modified from Berner, 2002) starting from the higher Late Permian values we suggest would result in an average global temperature of ~31°C with CO_2 values at ~40× modern levels, in reasonable agreement with our estimates of ~30°C (40° at the equator and 20° at the poles) and 30× modern CO_2. The above calculations assume that CO_2 was the sole greenhouse gas. Values would be lower if methane were abundant (e.g. Erwin, 1993; Krull and Retallack, 2000; Krull et al., 2000; Sheldon and Retallack, 2002). The 40° temperature is an assumed end-member value used to construct an extreme scenario and its consequences. Some of the most extreme summer heat probably occurred within three mid-latitude embayments in the Pangaean margin (our Fig. 1 and

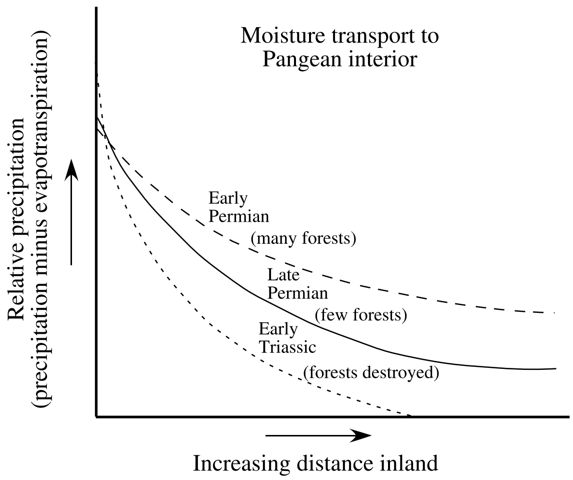

Fig. 7. Postulated decline in moisture transport to continental interiors from Early Permian to Early Triassic. Without abundant forests to serve as a terrestrial moisture supply, cyclonic storms would not penetrate as far into the Pangaean supercontinent despite their size in the Late Permian and Early Triassic. By Early Triassic, most rain would run off to oceans without reaching far into the continent.

figs. 2, 10, and 11 of Wignall and Twitchett, 2002) and fig. 1 of Wignall and Newton (2003) that are also likely sources for WSBW. Such a high temperature would have been deadly, and if achievable, would have been a significant causative factor in the extinction.

3.2. Reorganization of atmospheric and thermohaline circulation

Changes in Permo-Triassic ocean circulation have been explored by previous workers, largely in attempts to explain anoxia. The combination of factors we suggest for reorganization of thermohaline circulation not only provides potential solutions to problems of maintaining warm poles, but are consistent with anoxia generation. Ocean stratification (e.g. Holser, 1984; Wignall and Twitchett, 1996; Wignall and Newton, 2003) to produce anoxia has been suggested, as has weakened pole-driven thermohaline circulation and the effects of sinking water in a world with a low-oxygen atmosphere (Hotinski et al., 2000, 2001), but these changes do not help generate poleward heat transport. Zhang et al. (2001) suggested sinking subtropical brines, but their model results led them to conclude that, although this mechanism could promote deep-ocean anoxia, it would be difficult to sustain. We suggest that weakening of pole-driven thermohaline circulation ('thermal mode' of Zhang et al., 2001) in the Late Permian gave way to deep-ocean circulation driven by sinking warm brines from the subtropics to the middle latitudes. We suggest that this 'haline mode' (Zhang et al., 2001) was less vigorous than the preceding 'thermal mode', but it was sustainable in the latest Permian and Early Triassic. If so, it played a key role in both poleward heat transport and anoxia generation.

Melting of the Gondwanan ice sheets weakened oceanic thermohaline circulation (Fig. 5) as polar waters warmed to the point at which the pole-driven component of Early Permian thermohaline circulation became significantly weakened in the Late Permian (e.g. Hotinski et al., 2001). A reduction in cold brine generation by freezing water would be a consequence of shrinking ice sheets, perhaps to only seasonal ice. As salinity falls from 35 practical salinity units (psu) toward 30 psu, the effect of temperature on water density becomes negligible in cool water (Hay et al., 1998). If ocean waters freshen enough, the sinking of polar waters that drive today's deep-ocean circulation would greatly diminish and perhaps cease because below a salinity of 24.7 psu, the densest seawater occurs at a temperature above the freezing point. Precipitation needed to sustain high-latitude forests (e.g. Taylor et al., 1992; Retallack, 1999) would perpetuate freshening of polar-ocean surface waters and prevent their sinking (Fig. 1).

Extensive Late Permian evaporite formation may have lowered ocean salinity (Beurlen, 1956; Fischer, 1964; Stevens, 1977; Lantzy, 1977; Holser, 1984). Surface salinity reduction from 35 psu to 30 psu has been invoked to stress stenohaline organisms to the point of elimination (Fischer, 1964; Stevens, 1977). Holser (1984) suggested that such a drop in surface salinity would lead to ocean stratification. Horita et al. (1991) used fluid inclusion data from evaporites to argue that the composition of Permian seawater is comparable (i.e. within about 5 psu) to that of today so that a 5-psu drop in surface salinity compared to modern values is within the limits of their measurement technique. Calculations using ice sheet melting generate a drop of 3 psu, and salt extraction by evaporite basins (2 psu) permits a surface salinity drop of 5 psu and a whole-ocean drop of 2 psu from Early Permian to Early Triassic (Table 2; Fig. 1). We do not claim that salinity changes *caused* extinction, but they would have affected surface-ocean stenohaline faunas. For instance, the low polar salinities that we postulate would deny most marine organisms a refugium from very high temperatures at low to mid-latitudes. However, tropical Permian holdover taxa did apparently find a temporary higher-latitude refugium where the peri-Gondwanan 'peninsular' and the Cimmerian terranes shielded Neotethys from hyposaline polar influx until their mid-Griesbachian extinction (Wignall and Newton, 2003). We suggest here that evaporation raised salinity of this higher latitude area to tolerable levels. In a world ocean with deep-water anoxia and euxinia, upwelling waters would have been anoxic, whereas surface waters in areas of sinking would contain significant, albeit low levels of atmosphere-derived oxygen. A strong candidate for such a scenario occurs in the Tibetan shelf sections of a peri-Gondwanaland peninsula that blocked incursion of polar low salinity waters into the newly opening Neotethys at paleolatitudes of $\sim$40°S (Wignall and Twitchett, 2002, their fig. 10) or $\sim$55° S (Wignall and Newton, 2003, their fig. 1) and created a refugium for stenohaline tropical marine species. The shelf was shallow, and well enough mixed to remain the only oxic shelf to persist into the early Scythian (Wignall and Twitchett, 2002, their fig. 10; Wignall and Newton, 2003, their fig. 1). Even if overall ocean salinity did not change much, regional sinking of warm saline water to the ocean bottom and heavy precipitation could have significantly altered ocean circulation and greatly affected marine organisms.

The expansion of desert belts and retreat of forests to high latitudes discussed earlier probably led to extensive drainage of mid-latitude aquifers that contributed to marine stratification. Even as monsoonal conditions strengthened in the Late Permian (Kutzbach and Gallimore, 1989; Parrish, 1993), tropical aquifers emptied because little of the monsoonal surface runoff across an unforested landscape percolated downward to recharge aquifers. Coastal relief resulting from the high freeboard of Pangaea at this time (Haq et al., 1987) probably facilitated aquifer drainage.

The expansion and intensification of mid-latitude evaporation (Fig. 1) probably strengthened evaporation-driven thermohaline circulation at middle latitudes. Fig. 5 illustrates our model progression by which evaporation-driven mid-latitude sinking began to compete with weakening, ice-free polar sinking (Hotinski et al., 2001) in the Late Permian. The time at which sinking warm brines began to be significant may have been in the mid-Late Permian when they supplanted upwelling in the embayment in which the Phosphoria Formation accumulated (e.g. Sheldon, 1989; Maughan, 1994; Stephens and Carroll, 1999). By latest Permian polar sinking ceased and was replaced by polar upwelling of WSBW that formed as the ‘haline mode’ of Zhang et al. (2001) became dominant.

Significant atmospheric consequences arise for a warm world with weak ocean circulation. Three aspects of the Permo-Triassic world support considerable alteration to the manner in which atmospheric circulation operated (Fig. 1). These are: (1) the need for increased atmospheric heat transport in light of equably warm global temperatures and weakened surface ocean circulation in the Late Permian and Early Triassic, (2) breakdown of Early Permian high pressure polar cells like those in the modern icehouse to provide the warmth and moisture at Late Permian and Early Triassic high paleolatitudes, and (3) expansion of the sinking dry air masses between the Permo-Triassic equivalents of the Hadley and Ferrel cells to paleolatitudes perhaps as high as 45° by the Early Triassic. We suggest that Late Permian to Middle Triassic desert belts (Ziegler et al., 1993, 1997) may have encompassed latitudes between 15° and 45°, perhaps ranging as high as 60° (Figs. 1, 5 and 6). Whether a three-cell-per-hemisphere system simply underwent a change in scale (Fig. 1B,C) or whether these cells broke up into a more chaotic system (Fig. 1C), remains an open question, but it does not directly affect our model. The moist climates required by the Late Permian high-latitude forests discussed earlier (Taylor et al., 1992; Retallack, 1999), preclude the dominance of high pressure (Fig. 1) that mandates dry climate and support weakening or breakdown of the polar cell.

The high atmospheric vapor resulting from increased evaporation of the oceans would serve as a positive feedback favoring further warming because water vapor is a more potent greenhouse gas than CO_2. Tropical and polar rainfall would likely have been more intense than in the modern world. With minimal forest cover, high runoff and mechanical erosion would prevail over chemical weathering, resulting in limited nutrient input to oceans.

Today’s surface oceans are responsible for about half of the poleward heat transport from the tropics (Wells, 1997). The weakened deep-ocean circulation suggested here and by previous workers (Holser, 1977, 1984) coupled with weaker surface currents that resulted from reduced pole-to-equator temperature gradients would have diminished the surface ocean's effectiveness at transporting heat from the tropics to the poles. If planetary windbelt velocities and dependent ocean surface current velocity decreased accordingly, deep-ocean heat transport and its mining by cyclonic storms would be left as the most logical way for poleward heat transport to increase.

3.3. Storm activity

Warming alone suggests increased tropical cyclone frequency and intensity (e.g. Marsaglia and Klein, 1983; Duke, 1985; Barron, 1989; Ito et al., 2001), and we apply this to the Late Permian and the Early Triassic (Fig. 5). However, warm waters in the deep ocean and at high paleolatitude would fuel particularly intense storm activity. Because cyclonic storms cause strong Ekman transport upwelling, cold water at depth and at high latitudes in the modern oceans limits cyclone size and confines them to the tropics (Wells, 1997). Like today, the growth of Early Permian cyclonic storms was probably stopped when they reached cold water at high paleolatitudes and at the $\sim$150-m-deep thermocline. Warm waters at depth in the Late Permian and Early Triassic (Figs. 5 and 8) would allow cyclonic storms to reach much deeper waters as they mined those waters for heat, generating exceptionally strong storms that could deliver surface heat and moisture to high paleolatitudes (Fig. 5). We assume that the new maximum depth for oceanic storm activity was where the sheer physical mass of water (not cold temperature) became the ultimate limit on hurricane growth. With no ice caps, it is conceivable that even polar waters might not have been cold enough to stop hurricanes, although they might have been cool enough to slow them down and weaken them while they remained in those waters, only to strengthen if they returned to lower paleolatitudes. It may have been possible for Late Permian and Early Triassic cyclonic storms to completely circumnavigate the weak oceanic gyres so that as long as these hurricanes and other cyclonic storms remained at sea, they could keep traversing the gyres and contributing to poleward surface heat transfer until stopped by extreme polar winter cold or by passing over large, dry landmasses.

A mostly vegetation-free Late Permian and Early Triassic Pangaea would probably have stopped hurricanes much more effectively than today or in the Early Permian despite our suggested increases in storm intensity and frequency (Fig. 7). The rate at which cyclonic storms weaken as they move over land depends on their ability to draw strength from terrestrial warmth and moisture, and how fast they proceed inland. Given the reductions in forestation discussed earlier, terrestrial moisture availability would have been minimal. Lessened planetary windbelt velocities (Table 2) would have decreased storm penetration into the large Pangaean interior. Intense, storm-generated rainfall in near-coastal regions would result in substantial flood runoff, which, given the minimal vegetation in the low to mid-latitudes, would result in a predominance of braided rivers in the Late Permian and Early Triassic. Ward et al. (2000) recently reported a sharp change from meandering to braided rivers across the Permo-Triassic boundary in the African Karoo sequence, and Early Triassic braided stream deposition replaced more channelized Late Permian flow in Australia (Michaelsen, 2002).

The reorganization of global heat transport discussed above (Figs. 1 and 5) implies the need for significant alteration of the balance between input of solar radiation and radiative heat loss from the Early Permian icehouse to the Early Triassic greenhouse climate (Fig. 6). Heat mining of deep polar waters by cyclonic-storm upwelling would produce vegetation-sustaining Early Triassic high-latitude rainy climates. Abundant cloud cover in the region characterized by the weakened to absent polar atmospheric circulation cell (Fig. 1) would trap heat and maintain polar warmth (Fig. 6). Increased tropical warming would also thicken cloud cover over low-latitude oceans, further trapping heat, but also inhibiting solar input, preventing extreme warmth (Fig. 6). The loss of all cloud cover over Early Triassic desert belts that had expanded to mid-latitudes would probably allow these latitudes to become the zones of maximum heat absorption and evaporation in Pangaean oceanic embayments (Fig. 1) in summer and maximum radiative heat loss during winter, usurping the heat loss role played by modern and Early Permian poles.

3.4. Anoxia

Widespread anoxia and euxinia straddles the Permo-Triassic boundary in shelf settings (Wignall and Hallam, 1992, 1993; Wignall and Twitchett, 1996, 2002) and is conspicuous in the few known deep-ocean records (Isozaki, 1997). Deep-water anoxia in the Late Permian to Early Middle Triassic may have lasted up to 20 Myr (Table 1, Fig. 2). Isozaki (1997) suggested that euxinic conditions may have persisted for 10 Myr (mid-late Changxingian through Griesbachian) within this interval (Table 1, Figs. 2 and 5). This euxinia is probably correlative with the widespread shelf euxinic conditions mentioned above (Wignall and Twitchett, 1996, 2002).

The anoxia and euxinia are a logical consequence of the reorganization of thermohaline circulation invoked to explain heat transport and maintenance of polar warmth. Deep-water anoxia developed gradually as thermohaline circulation reorganized and weakened during the Late Permian (Fig. 5). As the 'haline mode' (Zhang et al., 2001) became established, WSBW became the chief supplier of O_2 to the sea floor. Importantly, a warm saline deep ocean means that dissolved oxygen levels of deep-ocean waters would likely be quite low because principal loci for brine generation are areas of anti-estuarine circulation that are normally low in dissolved oxygen. Furthermore, warm surface water could have held only about half as much oxygen as cooler Early Permian surface waters (Hotinski et al., 2000). Additionally, low levels of Late Permian atmospheric O_2 (Berner and Canfield, 1989; Berner, 2001; Graham et al., 1995; Sheldon and Retallack, 2002), would have minimized O_2 availability to ocean waters in the first place, perhaps to as little as two-thirds of today's level (Hotinski et al., 2000). Thus, low atmospheric O_2 content combined with its low solubility in warm water could have resulted in one-third as much ($1/2 \times 2/3$) of Late Permian–Early Triassic O_2 delivery to the ocean compared to that of today or Early Permian. Weakening of the Zhang et al. (2001) 'thermal mode' of circulation (Hotinski et al., 2001) and its replacement by the weaker 'haline mode' would further minimize deep-ocean oxygen. The deep-water sections described from Japan by Isozaki (1997) show an upward progression from oxic to euxinic facies. Red and oxic bedded chert passes upward to gray, dysoxic bedded cherts. In the Wujiapingian, the cherts disappear and give way to laminated anoxic shale with abundant pyrite. Black, organic-rich claystone records mid-Changxingian euxinic conditions in which total organic carbon is on the order of 4–10%, and $\delta^{34}S$ gets about 20‰ lighter than in the underlying unit, indicating bacterial sulfate reduction.

Early Triassic gaps in chert (Erwin, 1993; Kidder and Erwin, 2001) as well as phosphorite (Trappe, 1994) are both consistent with the widespread anoxia that continued into the Early Triassic. Both gaps are likely a function of diminished nutrient input and upwelling intensity given the expected low levels of chemical rock weathering and weak wind-driven oceanic circulation. Reduced wind stress (Table 2) suggested by Zhang et al. (2001), and weakened wind-driven upwelling (Hotinski et al., 2000) have been used in model attempts to generate deep-ocean anoxia. That the extinction wiped out organisms that could assist in burial of phosphorus and silica is probably why the gaps did not begin in the Late Changxingian. If the chert gap resulted from nutrient limitation, a reduction in mass of radiolarian tests would be expected during the chert gap. Examples of test reduction exist (Racki and Cordey, 2000; Kozur, 1998; Wignall and Newton, 2003), but freshened surface waters would also favor test reduction as radiolarians strove to remain buoyant, if they could tolerate lowered salinities. A return to more robust radiolarian tests occurs in the Spathian (Yao and Kuwahara, 1997), when supplies of nutrients and silica recovered. The few Early Triassic phosphate occurrences noted by Trappe (1994) are small deposits that are restricted mostly to high paleolatitudes (Fig. 1). Trappe attributed the minimal phosphate deposition to low relative sea level which greatly reduced the amount of available shelf area for phosphate deposition, but this is inconsistent

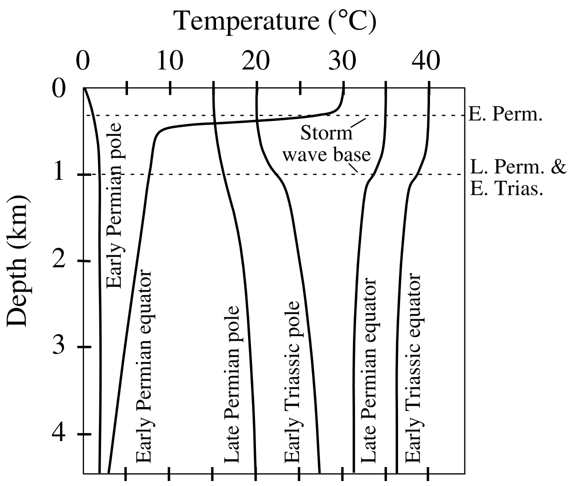

Fig. 8. Postulated thermoclines for the Early Permian, Late Permian, and Early Triassic based on the model maps in Fig. 1. Early Permian thermoclines would resemble those of the modern icehouse world, whereas the Late Permian and Early Triassic shold exhibit quite different thermoclines given the prediction of warm, saline bottom water. Storm wave base in the Early Permian should have been comparable to that of the modern icehouse. Storm wave base in the Late Permian and Early Triassic should have been deeper without shallow cold water to limit growth of cyclonic storms. The 1000-m suggestion on this figure is a crude estimate, and the Early Triassic storm wave base was probably deeper than the Late Permian one as suggested in Figure 5.

with the rapid transgression across the Permo-Triassic boundary (Table 1; Wignall and Hallam, 1992, 1993). If the Early Triassic ocean was vigorously circulating, more and richer phosphate deposits would be expected. The high-latitude occurrence of most of the few known low-grade phosphate deposits in the Early Triassic suggests those areas as sites where minor wind-driven upwelling could potentially tap more nutrient-rich waters.

4. Rapid events

4.1. Stable isotopes

Sulfate values of $\delta^{34}S$ shifted dramatically across the Permo-Triassic boundary (Fig. 9). The sharp increase began late in the Changxingian and continued through the Scythian (Claypool et al., 1980; Holser, 1988; Hallam and Wignall, 1997), as $\delta^{34}S$ rose from about +11‰, to more than +25‰ (Fig. 9).

Three explanations have been proffered for the $\delta^{34}S$ shift. Preferential removal of ^{32}S by burial in pyrite that formed via bacterial sulfate reduction would increase $\delta^{34}S$ in the evaporites (e.g. Hallam and Wignall, 1997; Broecker and Peacock, 1999). Alternatively, both Holser (1977) and Claypool et al. (1980) favored brine generation because they contended that the amount of pyrite genesis needed to bring about the shift was not achievable. Those authors did not perhaps anticipate the extensive nature of the euxinia and associated framboidal pyrite (Wignall and Twitchett, 2002) or the Siberian traps. Our model is consistent with increases in $\delta^{34}S$ being driven by both of these proposed mechanisms. We do not attempt to determine which may have been dominant. A third possibility for generation of the $\delta^{34}S$ anomaly is the release of mantle sulfur from a bolide impact (Kaiho et al., 2001), although Koeberl et al. (2002) questioned both the impact evidence and the $\delta^{34}S$ interpretations. We also point out that the $\delta^{34}S$ anomaly began before the rapid end-Permian extinction event and the suggested synchronous impact event.

We suggest that anti-estuarine circulation generated sinking brines at mid-latitude continental margins through much of the Late Permian. Hallam and Wignall (1997) argued against the brine mechanism by pointing out that what was probably the chief source of heavy brines in the Late Permian, the Zechstein Basin, was filled in before the end of the Permian. However, such basins tend to trap brines as evaporites rather than delivering $\delta^{34}S$-rich water to the deep sea. Erwin (1993) suggested that the global record of significant Late Permian evaporite genesis ended at about the beginning of the Changxingian (Fig. 2). Although spectacular evaporite-accumulating basins like the Zechstein Basin and the Delaware Basin were no longer active by the Changxingian, we speculate that intense, mid-latitude evaporation in a hot, dry world could generate brines along the outer edge of the exposed Late Permian Pangaean shelves (Fig. 1) and deliver warm, saline bottom water to the oceans. The associated

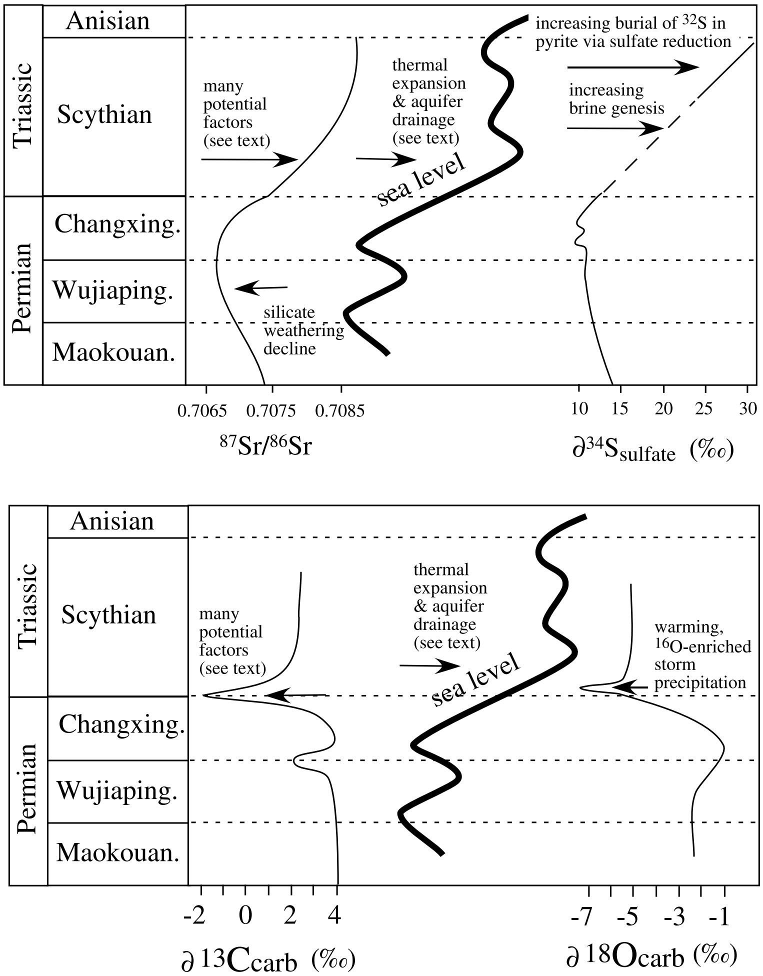

Fig. 9. Patterns of $^{87}Sr/^{86}Sr$, $\delta^{34}S$, $\delta^{13}C$, $\delta^{18}O$, and transgression across the Permo-Triassic boundary after Hallam and Wignall (1997). Suggested causes for each curve are highlighted on the diagrams, and more complete discussion of each is provided in the text.

downwelling would deliver nutrient-poor water to the deep sea.

Widespread euxinic waters should favor precipitation of small-diameter pyrite framboids in the water column (Wilkin et al., 1996; Wilkin and Barnes, 1997). Such framboids are common in the deeper-water Permo-Triassic section in Japan (Kajiwara et al., 1994). Wignall and Twitchett (2002) reported a distinct change from only a few large (~40 μm diameter) framboids in well-oxygenated and bioturbated muddy siltstones in the Late Permian of East Greenland upward into dark gray laminated muddy siltstones that bear the expected population of small framboids with diameters of mostly <6 μm.

A long-term Late Permian decline in $\delta^{13}C$ (Hallam and Wignall, 1997) is consistent with our predictions for long-term reductions in nutrients and productivity. A sharply negative excursion (Fig. 9) began just below the Permo-Triassic boundary at a number of sections (e.g. Holser et al., 1989; Gruszczynski et al., 1989; Magaritz et al., 1992; Bowring et al., 1998). This rapid drop from +2‰ to −2‰ may have occurred in less than 165 000 years in South China (Erwin et al., 2002) and perhaps lasted only tens of thousands of years (Bowring et al., 1998; Twitchett et al., 2001).

Attempts to balance the $\delta^{13}C$ budget have suggested contributions of many factors for generating the anomaly (e.g. Gruszczynski et al., 1989; Erwin, 1993; Broecker and Peacock, 1999; Wignall, 2001; Berner, 2002). Suggested inputs include volcanism, bicarbonate input from continental weathering, gas hydrates, and oxidation of biomass (e.g. Erwin, 1993; Wignall, 2001). Although the Siberian traps now appear to have been at least twice as large as previously thought (Reichow et al., 2002), they probably still failed to release enough CO_2 to generate the anomaly (Erwin, 1993; Wignall, 2001), particularly since much of the eruption post-dated the anomaly (Wignall, 2001). We suggest that rates of chemical weathering of continental rocks would be too slow to produce such a rapid $\delta^{13}C$ anomaly. However, release of characteristically $\delta^{13}C$-light gas hydrates could have constituted a significant component of the excursion, assuming suitable mechanisms existed to release them. High atmospheric methane in the Early Triassic has been suggested (Erwin, 1993; Morante, 1996; Krull and Retallack, 2000; Krull et al., 2000; Sheldon and Retallack, 2002). Deep-sea warming would favor hydrate release (e.g. Wignall, 2001; Bice and Marotzke, 2002).

Oxidation of living biomass as it went extinct would help lower overall $\delta^{13}C$ values, but not by enough to account for the anomaly (Erwin, 1993). Erosion of carbon exposed on the shelf before the extinction would be significant (Holser et al., 1989, 1991), but that would have taken place over a relatively long interval that preceded the $\delta^{13}C$ anomaly (Erwin, 1993). Berner (1989) suggested that in a warm, dry world burial rates of organic matter would be reduced because much dead biomass would oxidize before burial, but it does not explain the rapidity of the $\delta^{13}C$ shift.

Broecker and Peacock (1999) added that a shift from an efficient Permian food web to a less efficient Triassic one would have contributed to the anomaly by allowing increased burial of marine organic matter with sulfides. Such an inefficient system would probably increase phosphorus removal from the ocean, consistent with our low nutrient predictions. Berner's (2002) review of the anomaly reaffirms Erwin's (1993) suggestion that methane release was the most potent influence on the brief $\delta^{13}C$ anomaly, though other factors contributed as well. Berner (2002) favors a reorganization of the carbon cycle (Broecker and Peacock, 1999) and overall reductions in carbon burial.

Falling strontium isotopic ratios through the mid-late Permian to a Phanerozoic low in the latest Permian (Burke et al., 1982; Denison et al., 1994) are consistent with the declining relative continental influence (Table 1) and our suggested waning of silicate weathering as dry climates expanded on a fully assembled Pangaea. Our model suggests that the silicate weathering decline should have continued through the Early Triassic. However, the $^{87}Sr/^{86}Sr$ trend reversed itself (Fig. 9) and increased sharply in the Changxingian (Gruszczynski et al., 1989; Martin and Macdougall, 1995; Korte et al., 2003).

Existing explanations for the $^{87}Sr/^{86}Sr$ anomaly are problematic. A decline in mid-ocean ridge activity could account for the increase in the Sr ratio, but this is not presently testable. Intensification of terrestrial chemical weathering is a second hypothesis for the $^{87}Sr/^{86}Sr$ increase (Erwin, 1993; Martin and MccDougall, 1995). Higher levels of atmospheric water vapor and CO_2 and warmer temperatures would favor such weathering. However, significantly increased chemical weathering should have initiated cooling, which does not appear to have happened. Korte et al. (2003) suggested that widespread clastic sedimentation could have produced the anomaly, but detrital clastics are unlikely to have altered the signature preserved in biogenic carbonates and apatities unless the erosion of the source terranes from which those clastic sediments were derived exposed fresh silicate rock. On a fully sutured Pangaea, unroofing and exposure of ^{87}Sr-rich granite roots of the quiescent low-latitude orogenic belt (Fig. 1) may have tapped a radiogenic Sr hotspot analogous to that suggested for the modern Himalayan orogeny (e.g. Richter et al., 1992; Raymo, 1994), but whether such weathering of such granites took place fast enough to produce the anomaly is questionable. In our view, a satisfactory cause of the Sr-isotope anomaly is yet to emerge.

A sharp negative shift in $\delta^{18}O$ values in the Gartnerkofel core in the Austrian Alps (Holser et al., 1989) is consistent with warming by as much as 5°C that postdates the $\delta^{13}C$ discussed above (Fig. 9). Although oxygen isotope results are more commonly altered by diagenetic effects than those for carbon, the suggested warming is consistent with other evidence for warmth. The negative $\delta^{18}O$ spike could also reflect abundance of storm-generated meteoric water. The large cyclonic storms we propose would produce rainwater that is extremely light in $\delta^{18}O$ because rising of water vapor to the high altitudes common in such storm systems would intensively fractionate rainwater. That the $\delta^{18}O$ spike slightly follows the $\delta^{13}C$ anomaly is consistent with intensification of storms and warmth in the Early Triassic.

4.2. Transgression and rapid warming

A rapid third-order transgression (Hallam, 1989; Wignall and Hallam, 1992, 1993; Wignall and Twitchett, 1996) began in the early–mid Changxingian and continued across the Permo-Triassic boundary into the Scythian (Table 1, Fig. 9). Before this transgression flooded exposed Pangaean shelves, the ocean was at its lowest relative level in the Phanerozoic (Hallam, 1977; Vail et al., 1977). The magnitude of the transgression is estimated at just a few tens of meters (P. Wignall, pers. comm.). Smaller Late Permian landmasses were bounded by submerged shelf area while the Pangaean landmass was riding high (Hallam and Wignall, 1997). The spread of anoxia has been suggested as a possible cause of the marine portion of the Permo-Triassic extinction (Hallam, 1989; Wignall and Hallam, 1992, 1993; Wignall and Twitchett, 1996). Radiometric dates (Bowring et al., 1998) suggest that the entire Changxingian lasted only about 2 Myr. The Permian part of the transgression lasted perhaps only 1 Myr with the entire flooding event perhaps continuing for another million years into the Early Triassic (Erwin et al., 2002).

The cause of the transgression has so far remained unresolved. Tectonics have served as a default explanation for sea-level change, and have been suggested for this event (e.g. Hallam and Wignall, 1997). Although Hallam (1999) proffered the emplacement of a large igneous province as a possibility, no suitable tectonic event has yet been identified. Until evidence for such an event becomes available, other non-tectonic hypotheses should be considered.

We suggest that an intense thermal expansion of the world ocean for the last million years of the Permian and through the first million years of the Triassic offers a plausible non-tectonic mechanism. This mechanism may also apply to other transgression/anoxia/extinction events (e.g. Hallam and Wignall, 1999) in the geologic record for which no causal evidence of a transgression has been identified. Thermal expansion may explain up to half of the ~12-cm sea-level rise since the late 19th century, and it has been estimated that sea-level has fluctuated perhaps as much as 5 m during swings in deep-ocean temperature driven by Milankovitch cycles (Kump et al., 1999). We propose that WSBW finally and rapidly filled the deep ocean during the last million years of the Permian (Fig. 5) and corresponded to rapid intensification of global warming. Heating of Late Permian surface and deep-ocean waters could have thermally expanded them on a scale consistent with the few tens of meters (P.B. Wignall, pers. comm.) sea-level rise corresponding to the third-order transgression. Assuming an average whole-ocean temperature increase from a warm 15°C in the Late Permian to an extremely warm 30°C in the Early Triassic yields ~20 m of thermal expansion. The whole-ocean temperatures we use are simple averages of polar and equatorial shallow (upper 1 km) and deep (lower 3 km) temperatures in Fig. 1.

The 2 Myr 15°C rise in whole-ocean and Earth-surface temperature would probably trigger methane release from submarine gas hydrates (Dickens et al., 1995; Bice and Marotzke, 2002). The attendant release of extremely isotopically light carbon would explain the negative carbon isotope shift (Erwin, 1993) and also cause further warming atmospheric O_2 consumption as methane oxidized to CO_2. High-latitude global warming would wipe out the remaining cool-adapted glossopterid coal forests (Hallam and Wignall, 1999), causing further warming and O_2 lowering via the loss of their carbon burial function. The increase in fungal spores that peaks near the Permo-Triassic boundary (Visscher et al., 1996; Erwin et al., 2002) records non-combustive destruction of these latest Permian forests. The Siberian traps eruptions across the Permo-Triassic boundary (Erwin et al., 2002) contributed to further global warming via CO_2 emission and atmospheric O_2 consumption via oxidation of SO_2 emissions to sulfate that fueled the oceanic pyrite genesis that led to heavy Early Triassic $\delta^{34}S$ (e.g. Hallam and Wignall, 1997; Broecker and Peacock, 1999; Erwin et al., 2002; Wignall and Twitchett, 2002). Drainage of former coal forest aquifers would account for approximately 5 more meters of sea level rise based on modern figures (Sahagian et al., 1994; Berner and Berner, 1996), for a total rise of ~25 m.

The global warming and ocean volume expansion transgression would introduce new feedbacks into our model, including the sharp changes in sulfur and carbon isotopes. Solar heating of shallow waters on the newly flooded shelves would intensify already elevated cyclonic storm activity. The shallow shelf waters would be more susceptible to rapid salinity variation from the runoff generated by those storms. Warm, shallow, mid-latitude shelf waters would be even more readily evaporated than before, enhancing warm brine formation.

4.3. A proposed model for the extinction

The abrupt end-Permian extinction (Bowring et al., 1998) coincides with rapid $\delta^{13}C$ anomaly (e.g. Holser et al., 1989; Gruszczynski et al., 1989; Magaritz et al., 1992; Bowring et al., 1998). The extensive marine extinction (Erwin, 1993; Hallam and Wignall, 1997; Erwin et al., 2002) and terrestrial devastation (Retallack, 1995; Visscher et al., 1996; Hallam and Wignall, 1997) are correlative in East Greenland (e.g. Twitchett et al., 2001), but the extinction has also been suggested to be diachronous, occurring later in high latitudes (Wignall and Newton, 2003). Hallam and Wignall (1997) noted that the end-Permian extinction was the only major blow suffered by insects since their origin, and they suggested that the loss of insects was the reason why the zone of fungal enrichment (Visscher et al., 1996) that began about 1 Myr before the extinction (Erwin et al., 2002) is so conspicuous. Tracking of the forest loss by fungal spores in concert with the thermally induced transgression could reflect destruction of forests as global warming intensified and generated the transgression. Whatever the cause of the extinction, which now appears to have been diachronous (Wignall and Newton, 2003), the hot Late Permian climate combined with intense and frequent storms, salinity fluctuations, low atmospheric and oceanic oxygen levels, high sulfide levels, and limited availability of nutrients may explain why the rapid end-Permian extinction was so much worse than the sudden end-Cretaceous extinction, which occurred in a warm climate, but not one as unfavorable as the Late Permian.

Recent work by Becker et al. (2001) has revived interest in a bolide impact to explain the extinction. The search for direct evidence for the impact of an extraterrestrial body will undoubtedly continue, and until more unequivocal evidence is found, further debate will ensue. A bolide impact would certainly trigger numerous wide-ranging effects. However, we refrain from championing this mechanism because the results of Becker et al. (2001) have not yet been reproducible (Farley and Mukhopadhyay, 2001), and ongoing controversy regarding the placement of the boundary at the sampling site in Japan continues (Isozaki, 2001; Becker and Poreda, 2001). Other impact evidence discussed earlier (Kaiho et al., 2001) remains controversial (Koeberl et al., 2002).

As noted above, we suggest that as WSBW became established in the deep ocean, the heat caused not only thermal expansion and the transgression, but the warmer waters also released methane from sea-bottom clathrates that promoted further warming (e.g. Bice and Marotzke, 2002). Increased warming would sharply increase cyclonic storm activity, further contributing to methane release from ocean waters. Although we cannot prove that this effect of WSBW took place just prior to the extinction, it is tempting to suggest that it did because of the solutions it provides that have bearing upon the extinction and related events. Indeed, Erwin et al. (2002) suggested nine factors that must be accommodated in explanations of the extinction. An abbreviated version of their list includes: (1) widespread shallow- and deep-water anoxia; (2) the rapid marine and terrestrial $\delta^{13}C$ excursion that coincides with the boundary in the marine sections of China; (3) the temporal coincidence of the Siberian traps volcanism and the extinction; (4) the rapid (< 500 kyr) marine extinction and its occurrence during transgression; (5) absence of latest Permian glaciation; (6) evidence for rapid global warming at widely separated locations; (7) a rise in fungal spores over about 1 Myr leading up to the extinction; (8) controversial evidence for bolide impact; (9) the suggestion that shallow-marine ecosystems were disrupted after extinction-related changes in the deep ocean and in terrestrial ecosystems were already underway. Our model is consistent with all of these. Although it does not require a bolide impact, the rapid global warming is consistent with the effects of an impact should evidence for an extraterrestrial event become more concrete. Similarly, the timing of the Siberian traps eruptions also fit within the outline of our model. Though it is possible that the intense warming might have happened even without the eruptions, they undoubtedly contributed significantly.

5. The aftermath (and the recovery)

5.1. Delay

The unusually long Early Triassic recovery (Hallam, 1991) took at least twice as long as recoveries following other major extinctions (Erwin, 1998a,b). Although the scale of ecosystem devastation at the end of the Permian was clearly unprecedented in Earth history, we suggest that unfavorable climatic and oceanographic conditions contributed to delayed Early Triassic recovery, consistent with Hallam's (1991) suggestion that widespread anoxia perpetuated the delay.

The extinction itself would have severely affected the Earth system, and it probably intensified conditions that ultimately delayed the recovery. Some of the expected effects include: (1) addition of greenhouse gases to the atmosphere during decay of terrestrial biomass, but more importantly the loss of CO_2 drawdown capability suffered with land plant and ocean plankton extinctions, (2) a sharp decline in atmospheric oxygen driven by the decay of dead biomass and release of CH_4 from warming oceanic clathrates coupled with the sharp curtailment in photosynthetic production of oxygen, and (3) further reductions in nutrient availability when high-latitude forest destruction led to further reductions in silicate weathering.

The Early Triassic gaps discussed earlier help to frame the dire nature of the Early Triassic (Table 1, Fig. 2). The inability of the forests to recolonize mid- and low latitudes, as marked by the coal gap (Veevers et al., 1994; Retallack et al., 1996), assured the continuance of extreme aridity and warmth in these zones. Herbaceous lycopods were the dominant flora during the delayed recovery of the Early Triassic (Looy et al., 1999; Yaroshenko, 1997). Their role in photosynthetic CO_2 drawdown and burial was minimal compared to that of the preceding coal-generating forests. Similarly, their small root systems made them relatively ineffective catalysts for silicate weathering by reducing their mechanical weathering component and weakening their ability to retain local waters as effectively as the coal-generating coniferous forest ecosystems. Continuation of the orogeny gap (Table 1, Fig. 2) would also continue to depress nutrient mobilization and CO_2 drawdown.

The chert and phosphorite gaps (Erwin, 1993; Trappe, 1994) are consistent with the lack of a viable mechanism for concentrating nutrients. Wind-driven upwelling in the Early Triassic was probably weak because of reduced planetary wind velocities. Only limited amounts of nutrients were available at the depths tapped by upwelling. Deep-reaching cyclonic storms in our model would upwell great volumes of deep anoxic waters. Following the passage of storms, some upwelled nutrients would be temporarily available until local opportunistic dysoxic biotas (e.g. acritarchs) depleted the nutrient recycling loop by burying those nutrients in faecal matter and dead tissue. Lacking bioturbation, remobilization of those nutrients would be minimal. Such a system would favor dysoxic primary producers with dormant stages, such as acritarchs, that could wait out near-sterile conditions that mark the Early Triassic (Balme, 1970; Eshet, 1992). Short food chains/webs dominated by opportunistic taxa (Table 1) are consistent with the intermittent nutrient availability that we outline in an ocean that was probably anoxic to euxinic over wide areas at fairly shallow depths (Wignall and Twitchett, 2002). The reef gap (Fagerstrom, 1987) reflects the absence of framework- or mound-building metazoans, although small cyanobacterial reefs mark the Early Triassic (Schubert and Bottjer, 1992). As metazoan reefs typically thrive in stenohaline, nutrient-poor waters at stable temperatures (Wood, 1999), extreme warmth and/or storm- and monsoon-driven surface salinity oscillation would inhibit Early Triassic metazoan reef growth.

5.2. Recovery

Increased orogenic and floral contributions to silicate weathering and hence, CO_2 drawdown and rising nutrient availability in the mid-late Triassic (Table 1; Fig. 2) may have helped to fuel recovery. The onset of the high-latitude Yenshanian and Indosinian orogenies as South China and Cimmeria collided with Laurasia (Veevers, 1989) would have increased silicate weathering by exposing fresh, unweathered rock. The silicates in such a high-latitude orogeny would normally be expected to chemically weather only minimally (Moore and Worsley, 1994), but the abnormally warm and moist high paleolatitudes of the Early Triassic were probably effective sites for chemical weathering. Although denudation of the older high-latitude Uralian orogenic belt was probably still ongoing, it would not likely have been an effective chemical weathering contributor in the latest Permian and Early Triassic because the collisional convergent phase during which it would have been effective (if warm) was over. Coniferous forest recovery at the beginning of the Middle Triassic (Looy et al., 1999) probably increased photosynthetic CO_2 drawdown and intensified chemical weathering that released nutrients from terrestrial settings to the continents and oceans. Nutrient and oxygen availability probably also increased as sediment bioturbation resumed (Twitchett, 1999). As plankton capitalized on increased nutrients, photosynthetic oxygen production probably increased along with carbon burial, cooling, and the end of widespread anoxia and the phosphate and chert gaps. That recovery appears to have been initiated at high paleolatitudes (Wignall et al., 1998) is consistent with our predicted climate conditions that favor high-latitude refugia.

6. Tests of the model

A number of our model predictions are testable in the rock record. Frequent and intense cyclonic storms that formed most easily in the tropics and then traversed a wide range of latitudes while upwelling waters from a considerable oceanic depth are a key component of the model. We predict that the frequency, intensity, and maximum depth of Late Permian and Early Triassic storm deposits should be high, but also caution that frequency will be difficult to measure because large and frequent storms are likely to have eroded the deposits of preceding storms leaving an amalgamated record. Storm wave base is likely to have reached much deeper than the norm, and storm intensity was probably about as high any time in Earth history. The wavelength of hammocky cross-stratification may serve to test for intensity. Ito et al. (2001) linked this wavelength with modeled Mesozoic and Cenozoic CO_2 values. Their promising preliminary results suggest that a rise in storm intensity may match a model peak for CO_2 in the Cretaceous. Intense Early Triassic storm activity is consistent with unusual flat-pebble conglomerates reported by Wignall and Twitchett (1999), although lack of bioturbation also contributed to the origin of these deposits. Braided rivers should have become more common relative to meandering rivers from the equator to middle latitudes through the Late Permian as forests retreated from desert and monsoonal climates, and an abrupt rise of braided deposits to the dominant fluvial style should have marked the end-Permian devastation of terrestrial floras. Ward et al. (2000) have found this to be the case in the Karoo sequence in South Africa. They suggest that this might be a global pattern, and recent work by Michaelsen (2002) suggests a similar relationship in Australia. The few surviving Early Triassic radiolarian taxa would have faced serious limitations in nutrients, including silica. Silica-efficient radiolarian tests with reductions in the number, size, and thickness of spines, increased aperture diameter of pores, and an overall minimal volume are expected in the Early Triassic. Results from Racki and Cordey (2000), Kozur (1998) and Wignall and Newton (2003) support this test. Preservation of such gracile specimens is intrinsically difficult, and would be made even more so in a silica-deficient ocean. We suggest looking for them in and around the few low-grade Early Triassic phosphate deposits reported by Trappe (1994). Siliceous sponges would have been at least equally conservative in their use of silica. In the late Changxingian and early Griesbachian ocean characterized by widespread euxinia, populations of small pyrite framboids are expected to have been common, and have been reported from both deep (Kajiwara et al., 1994) and shallow (Wignall and Twitchett, 2002) deposits. Inclusion in future quantitative modeling of poleward warm deep-water transport and consequential increased storm transport of atmospheric latent heat and of polar heat trapping by clouds would serve as additional tests. Assuming that sinking warm brines is sustainable in ocean circulation modeling would test that factor.

7. Conclusions

Waning of the Alleghenian/Variscan/Hercynian orogeny may have been the initial cause of warming that set in motion a chain reaction of feedbacks that led continued warming via significant changes to Earth's atmosphere, biosphere, oceans, and terrestrial landscape. Conditions for life support were increasingly degraded on the Late Permian Earth, setting the stage for the extreme global warming and rapid, catastrophic extinction (e.g. Bowring et al., 1998; Erwin, 2002). The unusually long delay in post-extinction recovery (Hallam, 1991; Erwin, 1998a,b) probably resulted at least in part from the severity of the ecosystem collapse. However, the extinction itself probably intensified the already harsh conditions (e.g. low oxygen, high temperature, low nutrients), possibly contributing to the delay in recovery (e.g. Erwin et al., 2002). Our synthesis of a wide range of Permian and Triassic information and integration of that information with modeling results has yielded, in itself, a model for the evolution of the Permo-Triassic Earth system that raises several points for consideration in future models for climate change in this interval, as well as the extinction:

1. The necessity of continued poleward heat transport to maintain the warm, high-latitude climates suggested by available data requires consideration that sinking warm brines suggested by previous workers (Chamberlin, 1906; Brass et al., 2002; Zhang et al., 2001; Bice and Marotzke, 2002) were important. In the unusual latest Permian and Early Triassic greenhouse climate, the 'haline mode' may have been more sustainable than suggested by Zhang et al. (2001).
2. The loss or weakening of the thermocline and its replacement in some areas by a halocline above a warm and deep ocean would allow large cyclonic storms to mine heat from warm, deep waters. The ever larger storms would increase the role of the atmosphere in poleward latent heat transport.
3. The moist climates indicated by high-latitude Late Permian and Early Triassic vegetation suggests that the polar atmospheric circulation cells broke down or weakened. Cloud cover fed by condensing moisture released by the warm polar ocean would trap heat and maintain polar warmth and rainfall.
4. The changes in ocean circulation suggested for poleward heat transport also favor development of deep-ocean anoxia. Factors such as low atmospheric oxygen and weakened bottom water generation (e.g. Hotinski et al., 2000, 2001) as well as sinking warm brines (Zhang et al., 2001;

Bice and Marotzke, 2002) have been shown to be quantitatively somewhat weak in generating and maintaining deep-water anoxia when modeled individually. The combined effect of these multiple factors were probably able to achieve the widespread anoxia that is already well known (e.g. Wignall and Twitchett, 1996, 2002).

5. If WSBW rapidly expanded in the deep sea in the latest Permian as we suggest, it could have released ocean-water methane to intensify warming that not only caused the transgression, but also factored significantly in the extinction.

Acknowledgements

Discussions with D.H. Erwin, A. Hallam, and P.B. Wignall are appreciated. Thoughtful reviews by L.R. Kump and P.B. Wignall enabled us to focus our efforts much more effectively, and significantly improved the manuscript. Any errors are ours, not theirs.

References

Algeo, T.J., Berner, R.A., Maynard, J.B., Scheckler, S.E., 1995. Late Devonian oceanic anoxic events and biotic crises: 'rooted' in the evolution of vascular land plants? GSA Today 5, 45, 64–66.

Algeo, T.J., Scheckler, S.E., 1998. Terrestrial-marine teleconnections in the Devonian: Links between the evolution of land plants, weathering processes, and marine anoxic events. Philos. Trans. R. Soc. Lond. B 353, 113–130.

An, Z., Kutzbach, J.E., Prell, W.L., Porter, S.C., 2001. Evolution of Asian monsoons and phased uplift of the Himalaya-Tibetan plateau since Late Miocene times. Nature 411, 62–66.

Anbar, A.D., Knoll, A.H., 2002. Proterozoic ocean chemistry and evolution: A bioinorganic bridge? Science 297, 1137–1142.

Balme, B.E., 1970. Palynology of Permian and Triassic strata in the Salt Range and Surghar Range, West Pakistan. In: Kummel, B., Teichert, C. (Eds.), Stratigraphic Boundary Problems: Permian and Triassic of West Pakistan. University of Kansas, Lawrence, KS, pp. 305–453.

Barron, E.J., 1989. Severe storms during Earth history. Geol. Soc. Am. Bull. 101, 601–612.

Beauchamp, B., Baud, A., 2002. Growth and demise of Permian biogenic chert along northwest Pangea: Evidence for end-Permian collapse of thermohaline circulation. Palaeogeogr. Palaeoclimatol. Palaeoecol. 184, 37–63.

Becker, L., Poreda, R.J., 2001. An extraterrestrial impact at the Permian-Triassic boundary? Science 293, 2343a.

Becker, L., Poreda, R.J., Hunt, A.G., Bunck, T.E., Rampino, M., 2001. Impact event at the Permian-Triassic boundary: Evidence from extraterrestrial noble gases in fullerenes. Science 291, 1530–1533.

Beerling, D.J., Lomax, B.H., Royer, D.L., Upchurch, G.R.J., Kump, L.R., 2002. An atmospheric pCO_2 reconstruction across the Cretaceous-Tertiary boundary from leaf megafossils. Proc. Natl. Acad. Sci. 99, 7836–7840.

Bennett, S.C., 1996. Aerodynamics and thermoregulatory function of the dorsal sail of Edaphosaurus. Paleobiology 22, 496–506.

Berner, E.K., Berner, R.A., 1996. Global Environment: Water, Air, and Geochemical Cycles. Prentice Hall, New York, 376 pp.

Berner, R.A., 1989. Drying, O_2, and mass extinction. Nature 340, 603–604.

Berner, R.A., 1990. Atmospheric carbon dioxide levels over Phanerozoic time. Science 249, 1382–1386.

Berner, R.A., 1991. A model for atmospheric CO_2 over Phanerozoic time. Am. J. Sci. 291, 339–376.

Berner, R.A., 2001. Modeling atmospheric 0_2 over Phanerozoic time. Geochim. Cosmochim. Acta 65, 685–694.

Berner, R.A., 2002. Examination of hypotheses for the Permo-Triassic boundary extinction by carbon cycle modeling. Proc. Natl. Acad. Sci. 99, 4172–4177.

Berner, R.A., Canfield, D.E., 1989. A new model for atmospheric oxygen over Phanerozoic time. Am. J. Sci. 289, 333–361.

Beurlen, K., 1956. Der Faunenschnitt an der Perm-Trias Grenze. Zeitschr. Deutsch. Geol. Gesellsch. 108, 88–99.

Bice, K.L., Marotzke, J., 2002. Could changing ocean circulation have destabilized methane hydrate at the Paleocene/Eocene boundary? Paleoceanography 17, 8-1-8-13.

Bowring, S.A., Erwin, D.H., Jin, Y., Martin, M.W., Davidek, K.L., Wei, W., 1998. U/Pb zircon geochronology and tempo of the end-Permian mass extinction. Science 280, 1039–1045.

Brass, G.W., Southam, J.R., Peterson, W.H., 1982. Warm saline bottom water in the ancient ocean. Nature 296, 620–623.

Broecker, W., Peacock, S., 1999. An ecologic explanation for the Permo-Triassic carbon and sulphur isotope shifts. Glob. Biogeochem. Cycles 13, 1167–1172.

Burke, W.H. et al., 1982. Variation of seawater $^{87}Sr/^{86}Sr$ throughout Phanerozoic time. Geology 10, 516–519.

Canfield, D.E., 1998. A new model for Proterozoic ocean chemistry. Nature 396, 450–453.

Chamberlin, T.C., 1906. On a possible reversal of deep-sea circulation and its influence on geologic climates. J. Geol. 14, 363–373.

Claypool, G.E., Holser, W.T., Kaplan, I.R., Sakai, H., Zak, I., 1980. The age curves of sulfur and oxygen isotopes in marine sulfate, and their mutual interpretation. Chem. Geol. 28, 199–259.

Conaghan, P.J., Shaw, S.E., Veevers, J.J., 1994. Sedimentary evidence of the Permian/Triassic global crisis induced by the

Siberian hotspot, in: Embry, A.F., Beauchamp, B., Glass, D.J., (Eds.), Pangea: Global Environments and Resources. Volume Canadian Society of Petroleum Geologists Memoir 17, Calgary, AB, pp. 785–795.

Cook, P.J., McElhinny, P.J., 1979. A reevaluation of the spatial and temporal distribution of sedimentary phosphate deposits in the light of plate tectonics. Econ. Geol. 74, 315–330.

Crowell, J.C., 1999. Pre-Mesozoic Ice Ages: Their Bearing on Understanding the Climate System. Geological Society of America Memoir 192, Boulder, CO, 106 pp.

Delmelle, P., Stix, J., 2000. Volcanic Gases, in: Sigurdsson, H. (Eds.), Encyclopedia of Volcanoes. Academic Press, San Diego, CA, pp. 803–815.

Denison, R.E., Koepnick, R.B., Burke, W.H., Hetherington, E.A., Fletcher, A., 1994. Construction of the Mississippian, Pennsylvanian, and Permian $^{87}Sr/^{86}Sr$ curve. Chem. Geol. 112, 145–167.

Dickens, G.R., O'Neil, J.R., Rea, D.K., Owen, R.M., 1995. Dissociation of oceanic methane hydrate as a cause of the carbon-isotope excursion at the end of the Paleocene. Paleoceanography 10, 965–971.

Dickins, J.M., 1993. Climate of the Late Devonian to Triassic. Palaeogeogr. Palaeoclimatol. Palaeoecol. 100, 89–94.

Drever, J.I., 1994. The effect of land plants on weathering rates of silicate minerals. Geochim. Cosmochim. Acta 58, 2325–2332.

Duke, W.L., 1985. Hummocky cross-stratification, tropical hurricanes, and intense winter storms. Sedimentology 32, 167–194.

Ekart, D.D., Cerling, T.E., Montanez, I.P., Tabor, N.J., 1999. A 400 million year carbon isotope record of pedogenic carbonate: Implications for paleoatmospheric carbon dioxide. Am. J. Sci. 299, 805–827.

Erwin, D.H., 1993. The Great Paleozoic Crisis: Life and Death in the Permian. Columbia University Press, New York, 327 pp.

Erwin, D.H., 1994. The Permo-Triassic Extinction. Nature 367, 231–236.

Erwin, D.H., 1998a. After the End: Recovery from Extinction. Science 279, 1324–1325.

Erwin, D.H., 1998b. The end and the beginning: Recoveries from mass extinctions. Trends Ecol. Evol. 13, 344–349.

Erwin, D.H., Bowring, S.A., Jin, Y., 2002. End-Permian mass extinctions: A review, In: Koeberl, C., MacLeod, K.C. (Eds.), Catastrophic Events and Mass Extinctions: Impacts and Beyond. Special Paper 356 Geological Society of America, Boulder, CO, pp. 363–383.

Eshet, Y., 1992. The palynofloral succession and palynological events in the Permo-Triassic boundary interval in Israel. In: Sweet, W.C., Yang, Z., Dickins, J.M., Yin, H. (Eds.), Permo-Triassic Boundary Events in the Eastern Tethys. Cambridge University Press, Cambridge, pp. 134–145.

Fagerstrom, J.A., 1987. The Evolution of Reef Communities. John Wiley and Sons, New York, 600 pp.

Farley, K.A., Mukhopadhyay, S., 2001. An extraterrestrial impact at the Permian-Triassic boundary? Science 293, 2343a.

Fischer, A.G., 1964. Brackish oceans as the cause of the Permo-Triassic marine faunal crisis. In: Nairn, A.E.M. (Ed.), Problems in Palaeoclimatology. Proceedings of the NATO Palaeoclimates Conference, Newcastle Upon Tyne. Interscience Publishers, London, pp. 566–579.

Gibbs, M.T., Rees, P.M., Kutzbach, J.E., Ziegler, A.M., Behling, P.J., Rowley, D.B., 2002. Simulations of Permian climate and comparisons with climate-sensitive sediments. J. Geol. 110, 33–55.

Graham, J.B., Dudley, R., Aquilar, N.M., Gans, C., 1995. Implications of the late Palaeozoic oxygen pulse for physiology and evolution. Nature 375, 117–120.

Gruszcynski, M., Halas, S., Hoffman, A., Malkowski, K., 1989. A brachiopod calcite record of the oceanic carbon and oxygen isotope shifts at the Permian/Triassic transition. Nature 337, 64–68.

Haack, S.C., 1986. A thermal model of the sailback pelycosaur. Paleobiology 12, 450–458.

Hallam, A., 1977. Secular changes in marine inundation of USSR and North America through the Phanerozoic. Nature 269, 769–772.

Hallam, A., 1989. The case for sea-level change as a dominant causal factor in mass extinction of marine invertebrates. Philos. Trans. R. Soc. Lond. B 325, 437–455.

Hallam, A., 1991. Why was there a delayed radiation after the end-Palaeozoic extinctions? Hist. Biol. 5, 257–262.

Hallam, A., 1999. Discussion on ocean plateau formation: A cause of mass extinction and black shale deposition around the Cenomanian-Turonian boundary. J. Geol. Soc. Lond. 156, 208.

Hallam, A., Wignall, P.B., 1997. Mass Extinctions and Their Aftermath. Oxford University Press, Oxford, 320 pp.

Hallam, A., Wignall, P.B., 1999. Mass extinctions and sea-level changes. Earth Sci. Rev. 48, 217–250.

Haq, B.U., Hardenbol, J., Vail, P.R., 1987. Chronology of fluctuating sea levels since the Triassic. Science 235, 1156–1167.

Haupt, B.J., Seidov, D., 2001. Warm deep-water ocean conveyor during Cretaceous time. Geology 29, 295–298.

Hay, W.W., Wold, C.N., DeConto, R.M., 1998. The role of salinity in circulation of the Cretaceous ocean. Zent.bl. Geol. Paläontol. Teil I 11/12, 1445–1454.

Hein, J.R., Parrish, J.T., 1987. Distribution of siliceous deposits in space and time. In: Hein, J.R. (Ed.), Siliceous Sedimentary Rock-Hosted Ores and Petroleum. Van Nostrand Reinhold, New York, pp. 10–57.

Herbert, T.D., Sarmiento, J.L., 1991. Ocean nutrient distribution and oxygenation: limits on the formation of warm saline bottom water over the past 91 m.y. Geology 19, 702–705.

Holser, W.T., 1977. Catastrophic chemical events in the history of the ocean. Nature 267, 403–408.

Holser, W.T., 1984. Gradual and abrupt shifts in ocean chemstry during Phanerozoic time. In: Holland, H.D., Trendall, A.F. (Eds.), Patterns of Change in Earth Evolution. Springer-Verlag, Berlin, pp. 123–143.

Holser, W.T., 1988. Biogeochemical cycles of carbon and sulfur. In: Gregor, C.B., Garrells, R.M., Mackenzie, F.T., Maynard, J.B. (Eds.), Chemical Cycles in the Evolution of the Earth. John Wiley and Sons, New York, pp. 105–173.

Holser, W.T., Schönlaub, H.-P., Attrep, M., Jr., Boeckelmann, K., Klein, P., Magaritz, M., Orth, C.J., Fenninger, A., Jenny, C., Kralik, M., Mauritsch, H., Pak, E., Schramm, J.-M., Stattegger, K., Schmöller, R., 1989. A unique geochemical record at the Permian/Triassic boundary. Nature 337, 39–44.

Holser, W.T., Schönlaub, H.P., Boeckelmann, K., Magaritz, M., 1991. The Permian-Triassic of the Gartnerkofel-1 core (Carnic Alps, Austria): synthesis and conclusions. Abh. Geol. Bundesanst. 45, 213–232.

Horita, J., Friedman, T.J., Lazar, B., Holland, H.D., 1991. The composition of Permian seawater. Geochim. Cosmochim. Acta 55, 417–432.

Hotinski, R.M., Kump, L.R., Najjar, R.G., 2000. Opening Pandora's Box: The impact of open system modeling on interpretations of anoxia. Paleoceanography 15, 267–279.

Hotinski, R.M., Bice, K.L., Kump, L.R., Najjar, R.G., Arthur, M.A., 2001. Ocean stagnation and end-Permian anoxia. Geology 29, 7–10.

Isozaki, Y., 1997. Permo-Triassic boundary superanoxia and stratified superocean: Records from lost deep sea. Science 276, 235–238.

Isozaki, Y., 2001. An extraterrestrial impact at the Permian-Triassic boundary? Science 293, 2343a.

Ito, M., Ishigaki, A., Nishikawa, T., Saito, T., 2001. Temporal variation in the wavelength of hummocky cross-stratification: Implications for storm intensity through Mesozoic and Cenozoic. Geology 29, 87–89.

Kaiho, K. et al., 2001. End-Permian catastrophe by a bolide impact: Evidence of a gigantic release of sulfur from the mantle pages. Geology 29, 815–818.

Kajiwara, Y., Yamakita, S., Ishida, K., Ishiga, H., Imai, A., 1994. Development of a largely anoxic stratified ocean and its temporary massive mixing at the Permian/Triassic boundary supported by the sulfur isotopic record. Palaeogeogr. Palaeoclimatol. Palaeoecol. 111, 367–379.

Katz, M.E., Pak, D.K., Dickens, G.R., Miller, K.G., 1999. The source and fate of massive carbon input during the latest Paleocene thermal maximum. Science 286, 1531–1533.

Kidder, D.L., Erwin, D.H., 2001. Secular distribution of biogenic silica through the Phanerozoic: Comparison of silica-replaced fossils and bedded cherts at the series level. J. Geol. 109, 509–522.

King, G.M., 1990. Dicynodonts and the end Permian event. Palaeontol. Afr. 27, 31–39.

Knoll, A.H., Bambach, R.K., Canfield, D.E., Grotzinger, J.P., 1996. Comparative earth history and Late Permian mass extinction. Science 273, 452–457.

Koeberl, C., Gilmour, I., Reimold, W.U., Claeys, P., Ivanov, B., 2002. End-Permian catastrophe by bolide impact: Evidence of a gigantic release of sulfur from the mantle: Comment. Geology 30, 855–856.

Korte, C., Kozur, H.W., Bruckschen, P., Veizer, J., 2003. Strontium evolution of Late Permian and Triassic seawater. Geochim. Cosmochim. Acta 67, 47–62.

Kozur, H.W., 1998. Some aspects of the Permian-Triassic boundary (PTB) and the possible causes for biotic crises around this boundary. Palaeogeogr. Palaeoclimatol. Palaeoecol. 143, 227–272.

Krull, E.S., 1999. Permian palsa mires as paleoenvironmental proxies. Palaios 14, 530–544.

Krull, E.S., Retallack, G.J., 2000. $\delta^{13}C$ profiles from paleosols across the Permian-Triassic boundary: Evidence for methane release. Geol. Soc. Am. Bull. 112, 1459–1472.

Krull, E.S., Retallack, G.J., Campbell, H.J., Lyon, G.L., 2000. $\delta^{13}C_{org}$ chemostratigraphy of the Permian-Triassic boundary in the Maitai Group, New Zealand: Evidence for high-latitudinal methane release. New Zealand J. Geol. Geophys. 43, 21–32.

Kump, L.R., Kasting, J.F., Crane, R.G., 1999. The Earth System. Prentice-Hall, Inc., Upper Saddle River, New Jersey, 351 pp.

Kutzbach, J.E., Gallimore, R.G., 1989. Pangaean climates: Megamonsoons of the Megacontinent. J. Geophys. Res. 94, 3341–3357.

Kutzbach, J.E., Ziegler, A.M., 1993. Simulation of Late Permian climate and biomes with an atmosphere-ocean model: comparisions and observations. Philos. Trans. R. Soc. Lond. B 341, 327–340.

Lantzy, R.J., 1977. Catastrophe theory: Application to the Permian mass extinction. Geology 5, 724–728.

Looy, C.V., Brugman, W.A., Dilcher, D.L., Visscher, H., 1999. The delayed resurgence of equatorial forests after the Permian-Triassic ecologic crisis. Proc. Natl. Acad. Sci. 96, 13857–13862.

Magaritz, M., Krishnamurthy, R.V., Holser, W.T., 1992. Parallel trends in organic and inorganic carbon isotopes across the Permian/Triassic boundary. Am. J. Sci. 292, 727–739.

Makarenko, G.F., 1976. The epoch of Triassic trap magmatism in Siberia. Int. Geol. Rev. 19, 1089–1100.

Manabe, S., Stouffer, R.J., Spelman, M.J., 1994. Response of a coupled ocean-atmosphere model to increasing atmospheric carbon dioxide. Ambio 23, 44–49.

Marsaglia, K.M., Klein, G.D., 1983. The paleogeography of Paleozoic and Mesozoic storm depositional systems. J. Geol. 91, 117–142.

Martin, E.E., Macdougall, J.D., 1995. Sr and Nd isotopes at the Permian/Triassic boundary: A record of climate change. Chem. Geol. 125, 73–99.

Maughan, E.K., 1994. Phosphoria Formation (Permian) and its resource significance in the western interior, USA, in: Embry, A.F., Beauchamp, B., Glass, D.J. (Eds.), Pangea: Global Environments and Resources. Canadian Society of Petroleum Geologists Memoir 17, Calgary, pp. 479–495.

McRoberts, C.A., 2001. Triassic bivalves and the initial marine Mesozoic revolution: A role for predators? Geology 29, 359–362.

Michaelsen, P., 2002. Mass extinction of peat-forming plants and the effect on fluvial styles across the Permian-Triassic boundary, northern Bowen Basin, Australia. Palaeogeogr. Palaeoclimatol. Palaeoecol. 179, 173–188.

Miller, M.F., Hasiotis, S.T., Babcock, L.E., Isbell, J.L., Collinson, J.W., 2001. Tetrapod and large burrows of uncertain origin in Triassic high paleolatitude floodplain deposits, Antarctic. Palaios 16, 218–232.

Montanez, I.P., Tabor, N.J., Ekart, D.D., Chaney, D., Collister, J.W., 2001. Were changes in Early Permian atmospheric PCO_2 levels and collapse of Gondwanan glaciation linked? Earth System Processes Programmes with Abstracts. Geological Society of America and Geological Society of London, 71.

Moore, T.L., Worsley, T.R., 1994. Orogenic enhancement of weathering and continental ice-sheet initiation. In: Klein, G.D. (Ed.), Pangaea: Paleoclimate, Tectonics, and Sedimentation During Accretion, Zenith, and Breakup of a Supercontinent. Geological Society of America Special Paper 288, Boulder, CO, pp. 75–89.

Morante, R., 1996. Permian and Early Triassic isotopic records of carbon and strontium in Australia and a scenario of events about the Permian-Triassic boundary. Hist. Biol. 11, 289–310.

Parrish, J.T., 1993. Climate of the supercontinent Pangaea. J. Geol. 101, 215–233.

Racki, G., Cordey, F., 2000. Radiolarian palaeoecology and radiolarites: is the present the key to the past? Earth Sci. Rev. 52, 83–120.

Raymo, M.E., 1991. Geochemical evidence supporting T.C. Chamberlin's theory of glaciation. Geology 19, 344–347.

Raymo, M.E., 1994. The Himalayas, organic carbon burial, and climate in the Miocene. Paleoceanography 9, 399–404.

Rees, P.M., Gibbs, M.T., Ziegler, A.M., Kutzbach, J.E., Behling, P.J., 1999. Permian climates: Evaluating model predictions using global paleobotanical data. Geology 27, 891–894.

Rees, P.M., Ziegler, A.M., Gibbs, M.T., Kutzbach, J.E., Behling, P.J., Rowley, D.B., 2002. Permian phytogeographic patterns and climate data/model comparisons. J. Geol. 110, 1–31.

Reichow, M.K., Saunders, A.D., White, R.V., Pringle, M.S., Al'Mukhamedov, A.I., Medvedev, A.I., Kirda, N.P., 2002. $^{40}Ar/^{39}Ar$ dates from the west Siberian basin: Siberian flood basalt province doubled. Science 296, 1846–1849.

Renne, P.R., Zichao, Z., Richards, M.A., Black, M.T., Basu, A.R., 1995. Synchrony and causal relations between Permian-Triassic boundary crises and Siberian flood basalt volcanism. Science 269, 1413–1416.

Retallack, G.J., 1995. Permian-Triassic crisis on land. Science 267, 77–80.

Retallack, G.J., 1999. Postapocalyptic greenhouse paleoclimate revealed by earliest Triassic paleosols in the Sydney Basin, Australia. Geol. Soc. Am. Bull. 111, 52–70.

Retallack, G.J., 2001. A 300-million-year record of atmospheric carbon dioxide from fossil plant cuticles. Nature 411, 287–290.

Retallack, G.J., Veevers, J.J., Morante, R., 1996. Global coal gap between Permian-Triassic extinction and Middle Triassic recovery of peat-forming plants. Geol. Soc. Am. Bull. 108, 195–207.

Richter, R.M., Rowley, D.P., DePaolo, D.J., 1992. Sr isotope evolution of seawater: The role of tectonics. Earth Planet. Sci. Lett. 109, 11–23.

Rodland, D.L., Bottjer, D.J., 2001. Biotic recovery from the end-Permian mass extinction: Behavior of the inarticulate brachiopod Lingula as a disaster taxon. Palaios 16, 95–101.

Sahagian, D.L., Schwartz, F.W., Jacobs, D.K., 1994. Direct anthropogenic contributions to sea level rise in the twentieth century. Nature 367, 54–57.

Saltzman, M.R., Gonzalez, L.A., Lohmann, K.C., 2000. Earliest Carboniferous cooling step triggered by the Antler orogeny? Geology 28, 347–350.

Sarmiento, J.L., Herbert, T.D., Toggweiler, J.R., 1988. Causes of anoxia in the world ocean. Glob. Biogeochem. Cycles 2, 115–128.

Schubert, J.K., Bottjer, D.J., 1992. Early Triassic stromatolites as post-mass extinction disaster forms. Geology 20, 883–886.

Scott, A.C., 2000. The pre-Quaternary history of fire. Palaeogeogr. Palaeoclimatol. Palaeoecol. 164, 281–329.

Sheldon, N.D., Retallack, G.J., 2002. Low oxygen levels in earliest Triassic soils. Geology 30, 919–922.

Sheldon, R.P., 1989. Phosphorite deposits of the Phosphoria Formation, western United States. In: Notholt, A.J.G., Sheldon, R.P., Davidson, D.F. (Eds.), Phosphate Deposits of the World, v. 2. Cambridge University Press, Cambridge, pp. 53–61.

Stallard, R.F., 1985. River chemistry, geology, geomorphology, and soils in the Amazon and Orinoco basins. In: Drever, J.I. (Ed.), The Chemistry of Weathering. D. Reidel Publishing Co., Boston, MA, pp. 293–316.

Stanley, S.M., 1984. Temperature and biotic crises in the marine realm. Geology 12, 205–208.

Stanley, S.M., 1988. Paleozoic mass extinctions: Shared patterns suggest global cooling as a common cause. Am. J. Sci. 288, 334–352.

Stanley, S.M., Yang, X., 1994. A double mass extinction at the end of the Paleozoic Era. Science 266, 1340–1344.

Stephens, N.P., Carroll, A.R., 1999. Salinity stratification in the Permian Phosphoria sea; a proposed paleoceanographic model. Geology 27, 899–902.

Stevens, C.H., 1977. Was development of brackish oceans a factor in Permian extinctions? Geol. Soc. Am. Bull. 88, 133–138.

Taylor, E.L., Taylor, T.N., Cúneo, N.R., 1992. The present is not the key to the past: A polar forest from the Permian of Antarctica. Science 257, 1675–1677.

Taylor, E.L., Taylor, T.N., Cúneo, N.R., 2000. Permian and Triassic high latitude paleoclimates: evidence from fossil biotas. In: Huber, B.T., MacLeod, K.G., Wing, S.L. (Eds.), Warm Climates in Earth History. Cambridge University Press, Cambridge, pp. 321–350.

Trappe, J., 1994. Pangaean phosphorites - ordinary phosphorites genesis in an extraordinary world? In: Embry, A.F., Beauchamp, B., Glass, D.J. (Eds.), Pangaea: Global Environments and Resources. Canadian Society of Petroleum Geologists, pp. 469–478.

Twitchett, R.J., 1999. Paleoenvironments and faunal recovery after the end-Permian mass extinction. Palaeogeogr. Palaeoclimatol. Palaeoecol. 154, 27–37.

Twitchett, R.J., Looy, C., Morante, R., Visscher, H., Wignall, P.B., 2001. Rapid and synchronous collapse of marine and terrestrial ecosystems during the end-Permian biotic crisis. Geology 29, 351–354.

Vail, P.R., Mitchum, R.M., Thompson, S., 1977. Seismic stratigraphy and global changes of sea level. In: Payton, C.E. (Ed.), Seismic Stratigraphy - Applications to Hydrocarbon Exploration. American Association of Petroleum Geologists, Tulsa, pp. 83–97.

Valentine, J.W., Moores, E.M., 1970. Plate-tectonic regulation of faunal diversity and sea level: a model. Nature 228, 657–659.

Van Cappellen, P., Ingall, E.D., 1994. Benthic phosphorus regeneration, net primary production, and ocean anoxia: A model of the coupled marine biogeochemical cycles of carbon and phosphorus. Paleoceanography 9, 677–692.

Veevers, J.J., 1989. Middle/Late Triassic (230 ± 5) singularity in the stratigraphic and magmatic history of the Pangaean heat anomaly. Geology 17, 784–787.

Veevers, J.J., Conaghan, P.J., Shaw, S.E., 1994. Turning point in Pangaean environmental history at the Permian/Triassic (P/Tr) boundary. In: Klein, G.D. (Ed.), Pangaea: Paleoclimate, Tectonics, and Sedimentation During Accretion, Zenith, and Breakup of a Supercontinent. Geological Society of America, Boulder, CO, pp. 187–196.

Visscher, H. et al., 1996. The terminal Paleozoic fungal event: Evidence of terrestrial ecosystem destabilization and collapse. Proc. Natl. Acad. Sci. USA 93, 2155–2158.

Wang, Z., 1993. Evolutionary ecosystem of Permian-Triassic red beds in N. China: A historical record of natural global desertification In: Lucas, S.G., Morales, M. (Eds.), The Nonmarine Triassic. Bulletin of the New Mexico Museum of Natural History and Science 3, pp. 471–476.

Wang, Z., 2000. Vegetation on the eve of the P-T event in North China and plant survival strategies: An example of Upper Permian refutium in northwestern Shanxi. China Acta Palaeontol. Sin. Suppl. 39, 127–153.

Ward, P.D., Montgomery, D.R., Smith, R., 2000. Altered river morphology in South Africa related to the Permian-Triassic extinction. Science 289, 1740–1743.

Wells, N., 1997. The Atmosphere and Ocean: A Physical Introduction. John Wiley and Sons Ltd, Chichester, 394 pp.

Wignall, P.B., 2001. Large igneous provinces and mass extinctions. Earth Sci. Rev. 53, 1–33.

Wignall, P.B., Hallam, A., 1992. Anoxia as a cause of the Permian/Triassic mass extinction from northern Italy and the western United States. Palaeogeogr. Palaeoclimatol. Palaeoecol. 93, 21–46.

Wignall, P.B., Hallam, A., 1993. Griesbachian (Earliest Triassic) palaeoenvironmental changes in the Salt Range, Pakistan and southeast China and their bearing on the Permo-Triassic mass extinction. Palaeogeogr. Palaeoclimatol. Palaeoecol. 102, 215–237.

Wignall, P.B., Twitchett, R.J., 1996. Oceanic Anoxia and the End Permian Mass Extinction. Science 272, 1155–1158.

Wignall, P.B., Twitchett, R.J., 1999. Unusual intraclastic limestones in Lower Triassic carbonates and their bearing on the aftermath of the end-Permian mass extinction. Sedimentology 46, 303–316.

Wignall, P.B., Twitchett, R.J., 2002. Extent, duration, and nature of the Permian-Triassic superanoxic event, in: Koeberl, C., MacLeod, K.C. (Eds.), Catastrophic Events and Mass Extinctions: Impacts and Beyond, Special Paper 356. Geological Society of America, Boulder, CO, pp. 395–413.

Wignall, P.B., Newton, R., 2003. Contrasting deep-water records from the Upper Permian and Lower Triassic of South Tibet and British Columbia: Evidence for a diachronous mass extinction. Palaios 18, 153–167.

Wignall, P.B., Morante, R., Newton, R., 1998. The Permo-Triassic transition in Spitsbergen: δ^{13}Corg chemostratigraphy, Fe and S geochemistry, facies, fauna and trace fossils. Geol. Mag. 135, 47–62.

Wilkin, R.T., Barnes, H.L., 1997. Formation processes of framboidal pyrite. Geochim. Cosmochim. Acta 61, 323–339.

Wilkin, R.T., Barnes, H.L., Brantley, S.L., 1996. The size distribution of framboidal pyrite in modern sediments: An indicator of redox conditions. Geochim. Cosmochim. Acta 60, 3897–3912.

Windley, B.F., 1995. The Evolving Continents. John Wiley and Sons, New York, 526 pp.

Wood, R., 1999. Reef Evolution. Oxford University Press, Oxford, 414 pp.

Worsley, T.R., Kidder, D.L., 1991. First-order coupling of paleogeography and CO_2 with global surface temperature and its latitudinal contrast. Geology 19, 1161–1164.

Yao, A., Kuwahara, K., 1997. Radiolarian faunal change from Late Permian to Middle Triassic times. News Osaka Micropaleontol. Spec. Vol. 10, 87.

Yaroshenko, O.P., 1997. Palynology and phytogeography of the Early Triassic. Paleontol. J. 31, 168–177.

Zachos, J.C., Lohmann, K.C., Walker, K.C.G., Wise, S.W., 1993. Abrupt climate changes and transient climates during the Paleogene: A marine perspective. J. Geol. 101, 191–213.

Zhang, R., Follows, M.J., Grotzinger, J.P., Marshall, J., 2001. Could the Late Permian deep ocean have been anoxic? Paleoceanography 16, 317–329.

Ziegler, A.M., Warm polar currents: Eos: Trans. Am. Geophys. Union, Spring Meeting 98 suppl. S50.

Ziegler, A.M., Parrish, J.M., Jiping, Y., Gyllenhaal, E.D., Rowley, D.B., Parrish, J.T., Shangyou, N., Bekker, A., Hulver, M.L., 1993. Early Mesozoic phytogeography and climate. Philos. Trans. R. Soc. Lond. B 341, 297–305.

Ziegler, A.M., Hulver, M.L., Rowley, D.B., 1997. Permian world topography and climate. In: Martini, I.P. (Ed.), Late Glacial and Postglacial Environmental Changes - Quaternary, Carboniferous-Permian, and Proterozoic. Oxford University Press, Oxford, pp. 111–146.